Electronic Supplementary Information (ESI)

Post-Polymerisation Modification of Poly(3-hydroxybutyrate) (PHB) using Thiol-ene and Phosphine Addition

Lucas Al-Shok,[a] James S. Town,[a] Despina Coursari,[a] Paul Wilson,[a] David M. Haddleton*[a]

a. Department of Chemistry, University of Warwick, Coventry, CV4 7AL, UK. E-mail: d.m.haddleton@warwick.ac.uk

1 Data

1.1 NMR of starting materials

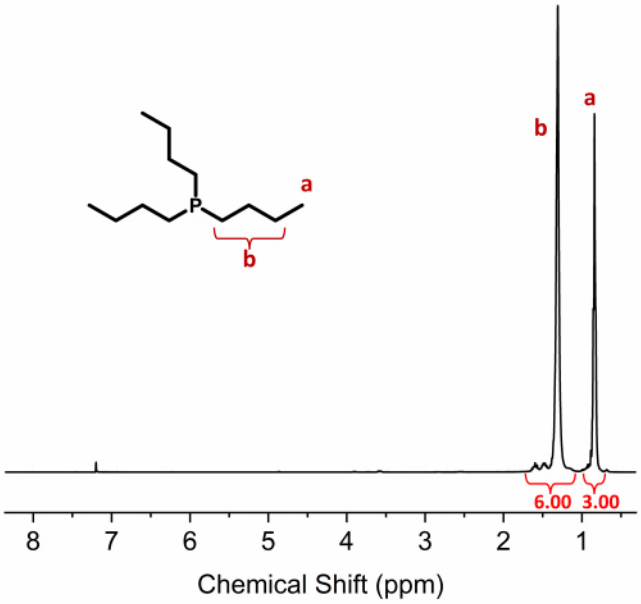

Figure S1: ^{1}H-NMR spectrum (400 MHz. $CDCl_3$) of tributylphosphine.

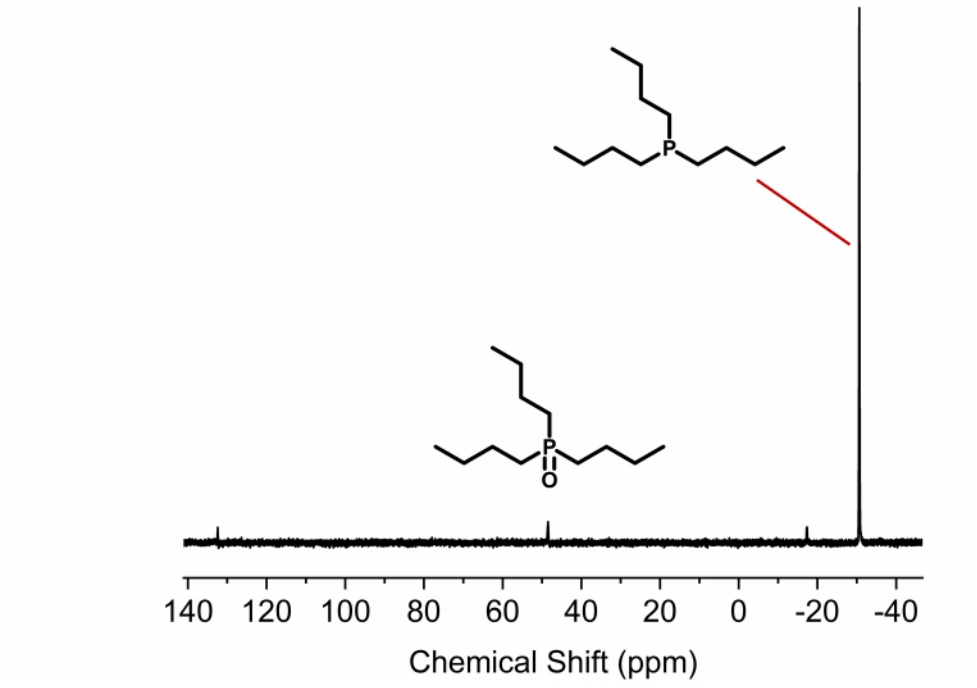

Figure S2: ^{31}P NMR spectrum (162 MHz, $CDCl_3$) of tributylphosphine.

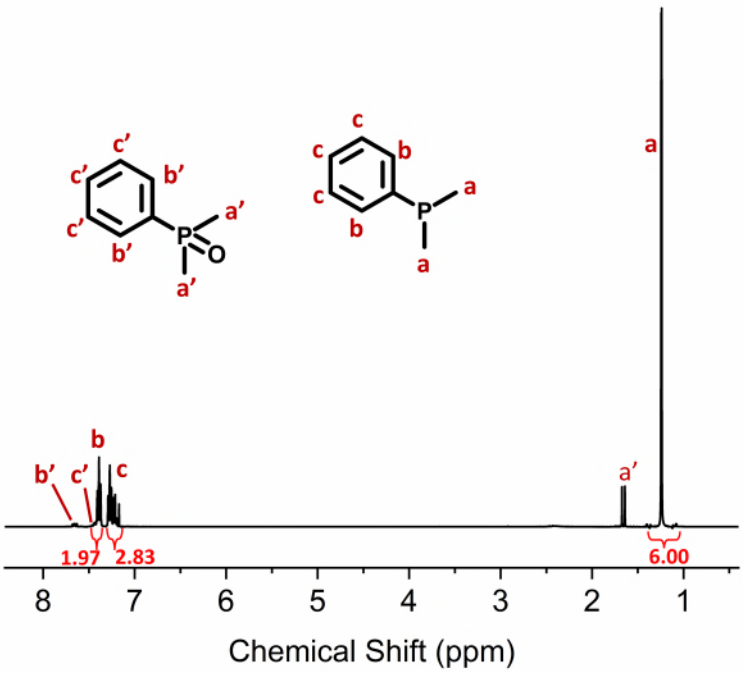

Figure S3: ^{1}H NMR spectrum (400 MHz, $CDCl_3$) of dimethylphenylphospine.

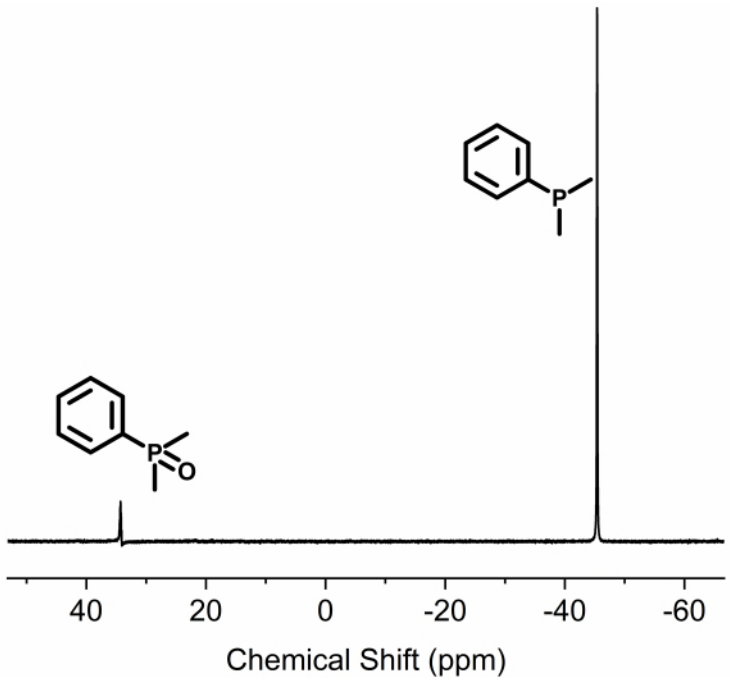

Figure S4: ^{31}P NMR spectrum (162 MHz, $CDCl_3$) of dimethylphenylphosphine.

1.2 Polymer-Synthesis

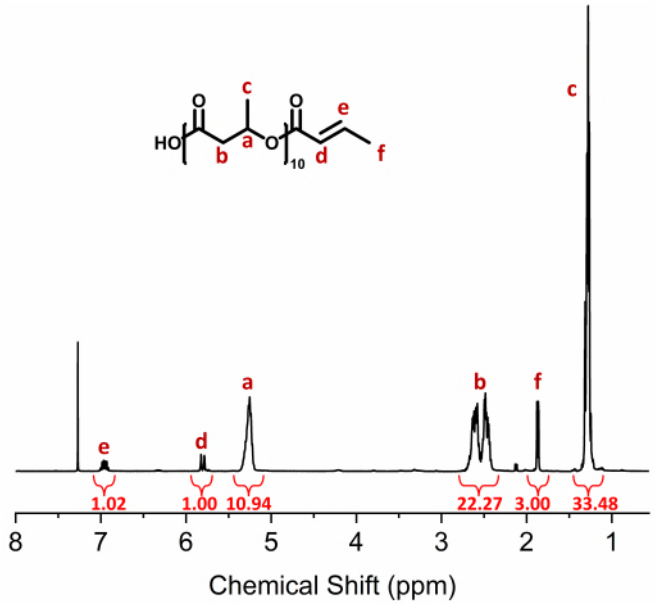

Figure S5: ^{1}H NMR spectrum (400 MHz, $CDCl_3$) of low molecular weight PHB.

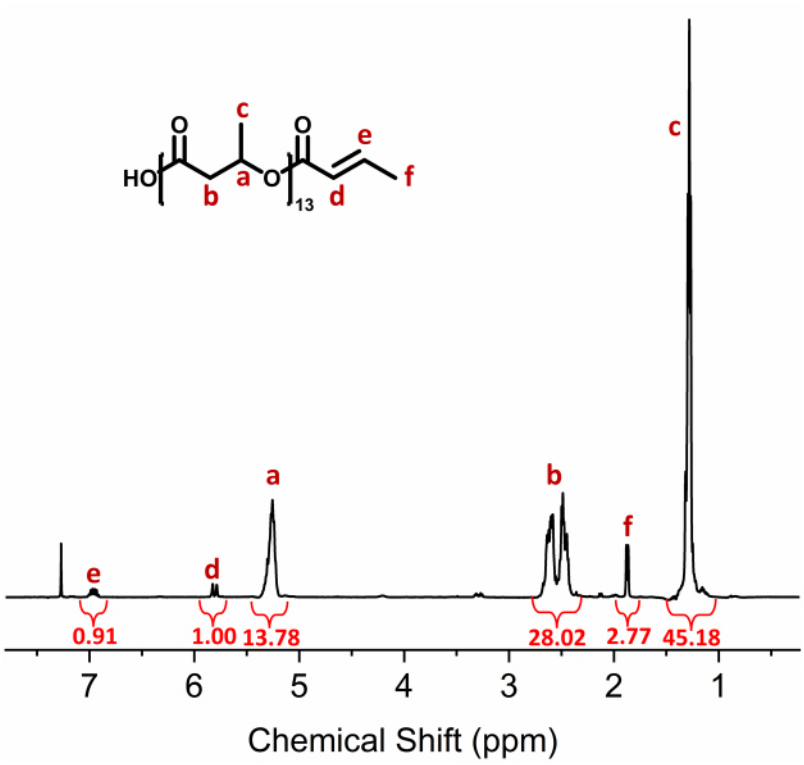

Figure S6: ^{1}H NMR spectrum (400 MHz, $CDCl_3$) of medium molecular weight PHB.

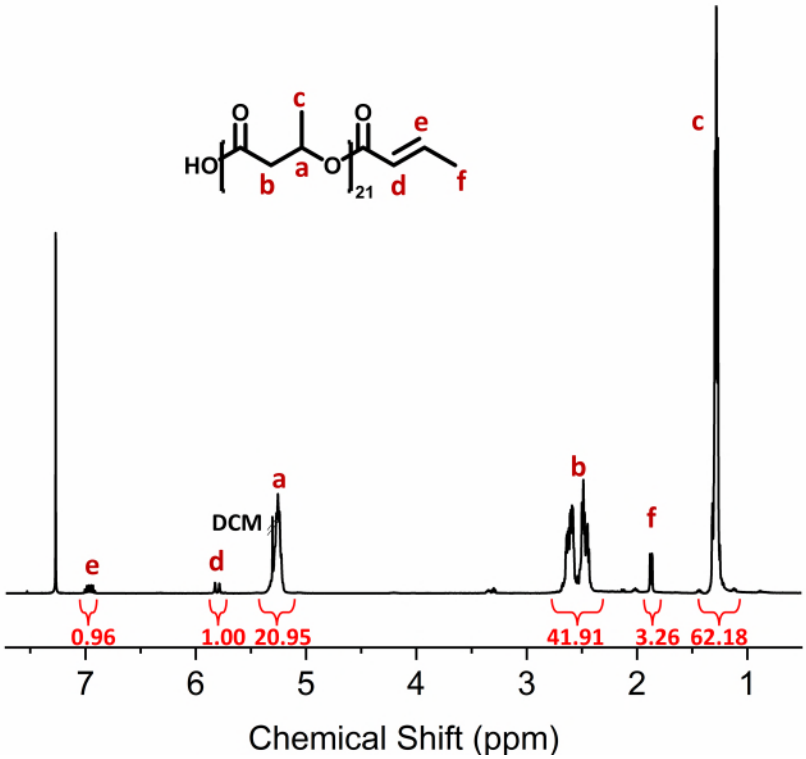

Figure S7: ^{1}H NMR spectrum (400 MHz, $CDCl_3$) of medium-high molecular weight PHB.

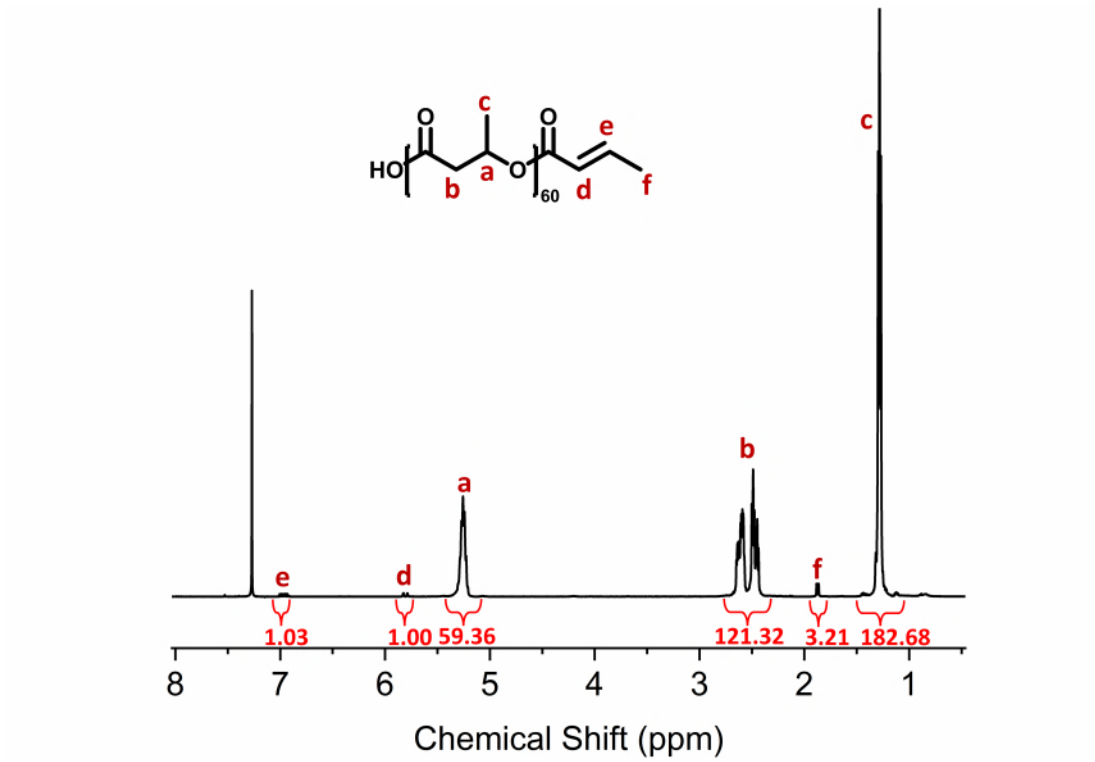

Figure S8: ^{1}H NMR spectrum (400 MHz, $CDCl_3$) of high molecular weight PHB.

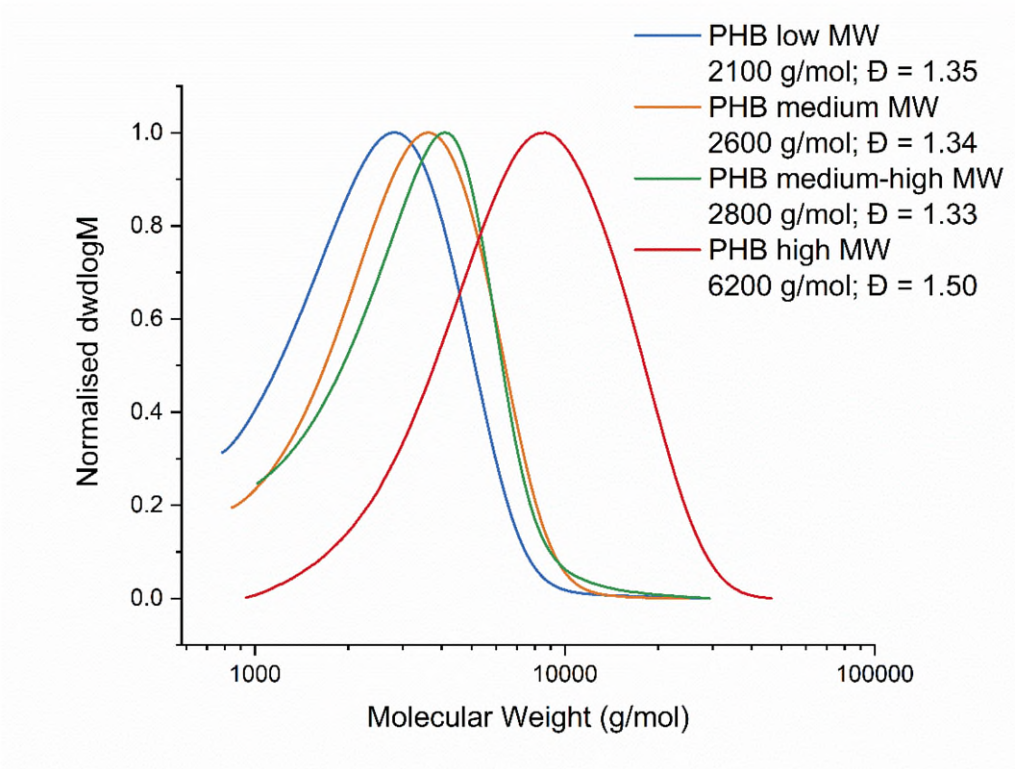

Figure S9: Size-exclusion chromatogram showing distributions of molecular weights of synthetic PHB.

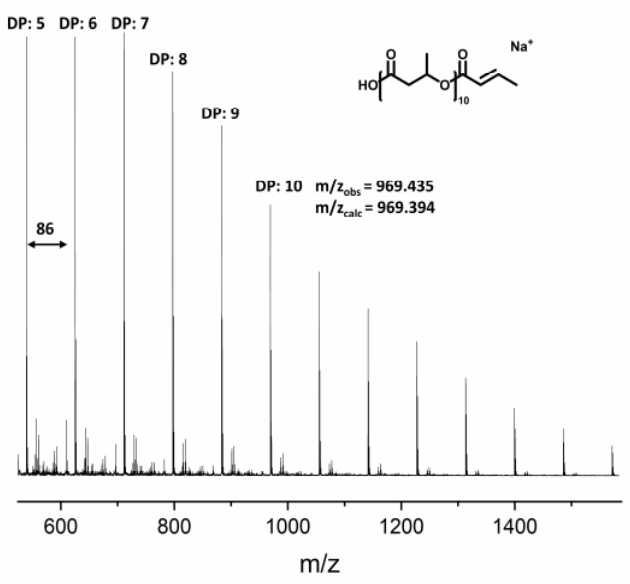

Figure S10: MALDI-ToF spectrum of low molecular weight PHB, measured via reflectron positive ion mode.

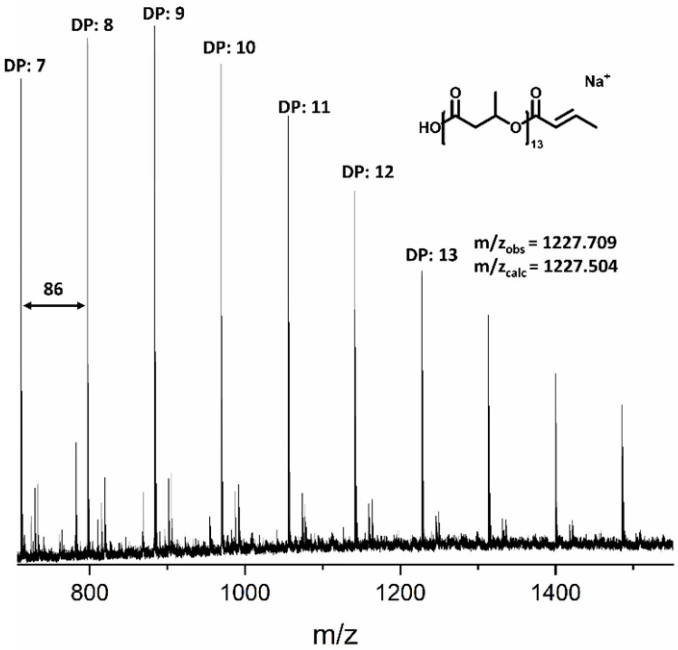

Figure S11:MALDI-ToF spectrum of medium molecular weight PHB, measured via reflectron positive ion mode.

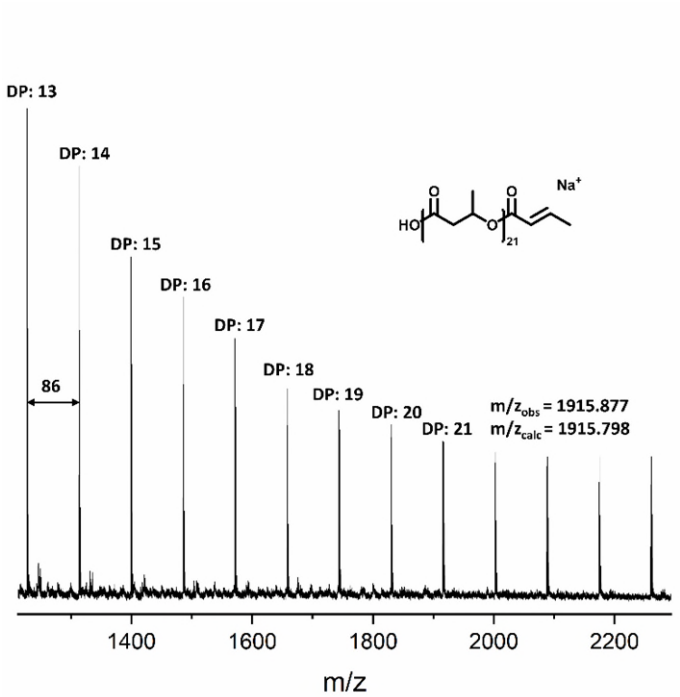

Figure S12: MALDI-ToF spectrum of medium-high molecular weight PHB, measured via reflectron positive ion mode.

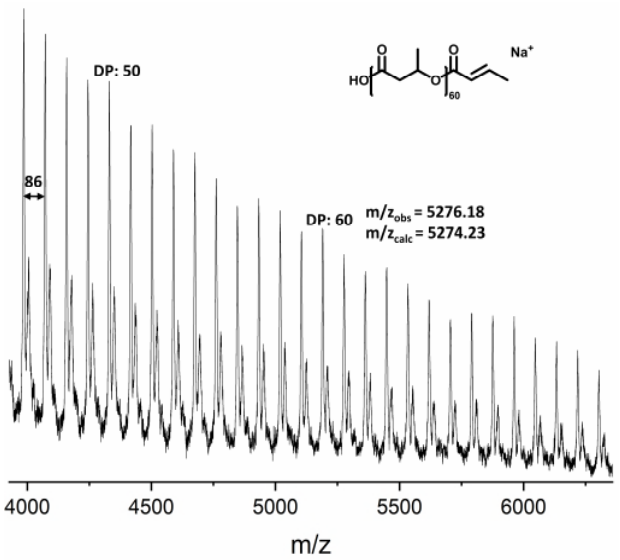

Figure S13: MALDI-ToF spectrum of high molecular weight PHB, measured via linear positive ion mode.

1.3 Polymer Functionalisation

Low molecular weight PHB

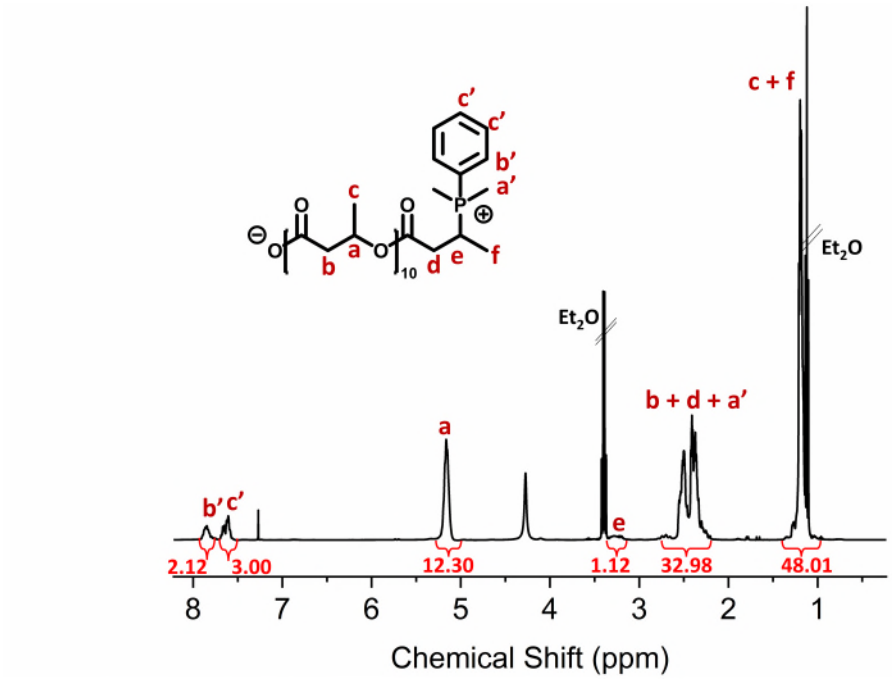

Figure S14: ^{1}H-NMR (400 MHz, $CDCl_3$) of low molecular weight PHB functionalised with DMPP.

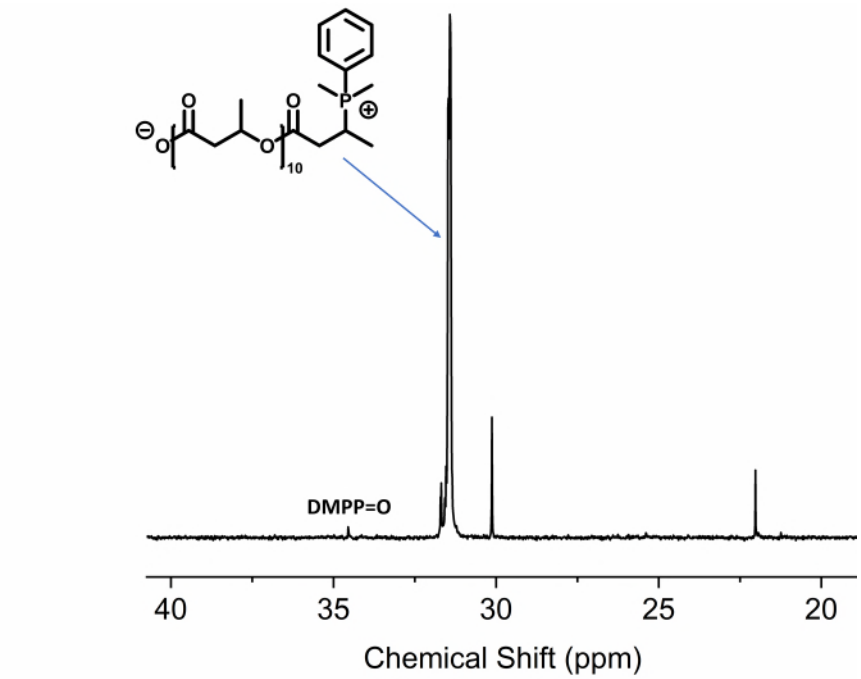

Figure S15: ^{31}P-NMR (162 MHz, $CDCl_3$) of low molecular weight PHB functionalised with DMPP.

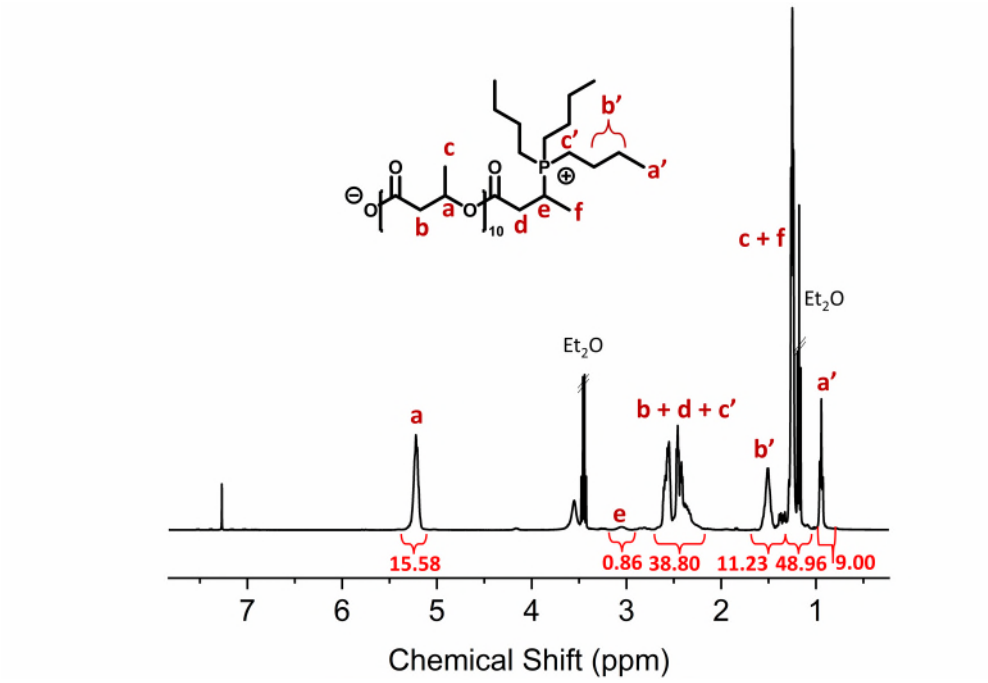

Figure S16: ^{1}H-NMR (400 MHz. $CDCl_3$) of low molecular weight PHB functionalised with Bu_3P.

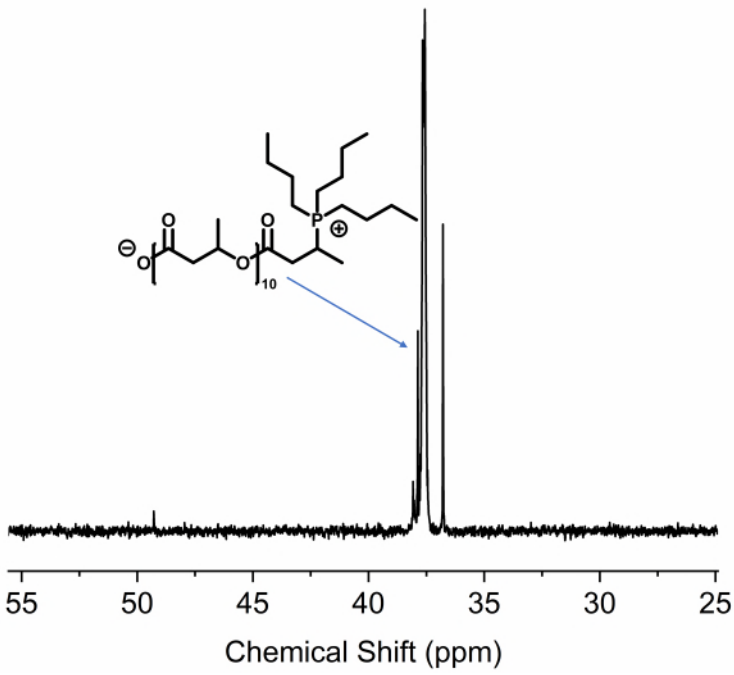

Figure S17: ^{31}P-NMR (162 MHz $CDCl_3$) of low molecular weight PHB functionalised with Bu_3P.

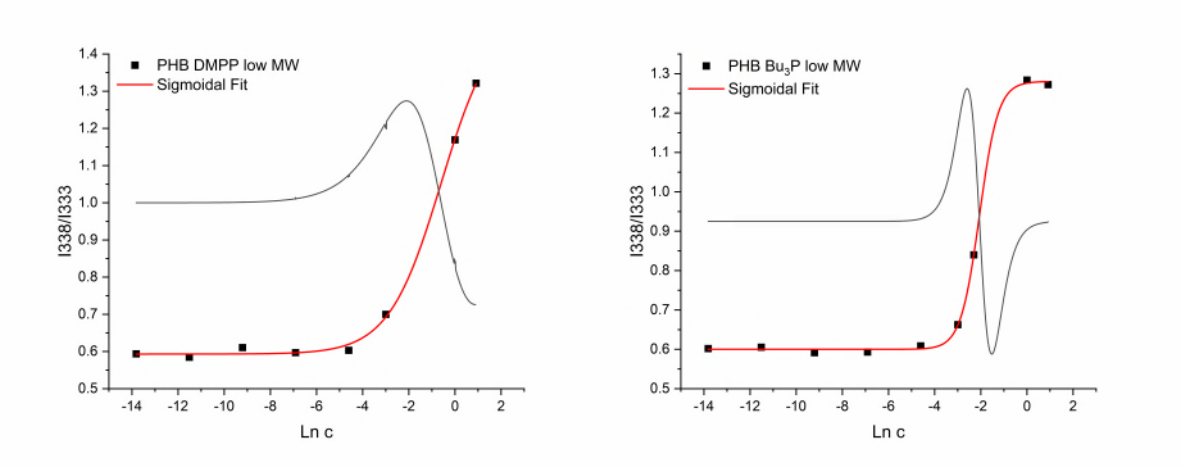

Figure S18: Plots of the relationship between fluorescence emission at 338 nm and 333 nm with a logarithmic concentration, measured for different low molecular weight polymer adduct concentrations in the presence of pyrene. PHB DMPP (left), PHB Bu_3P (right).

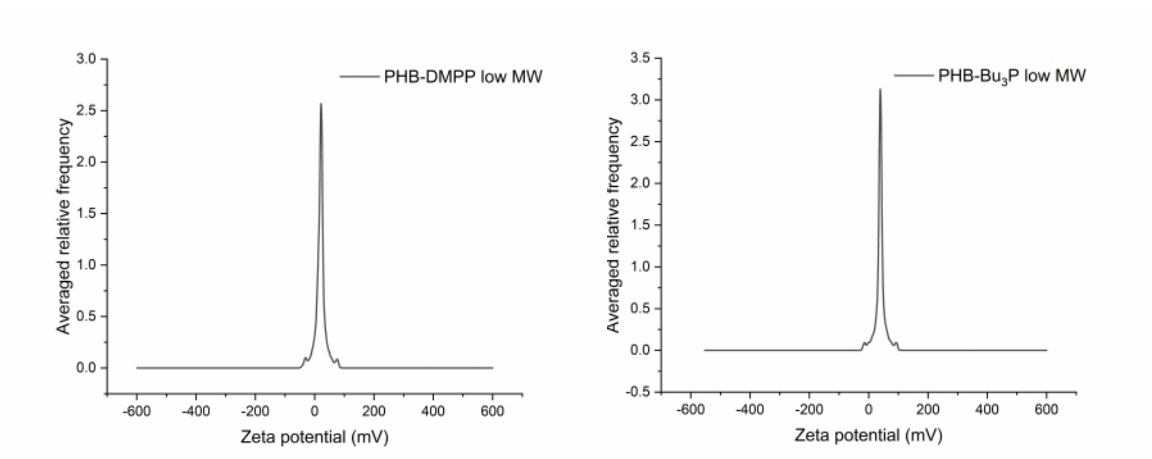

Figure S19: Zeta potential recorded for low molecular weight PHB functionalised with DMPP (left) and Bu_3P (right), respectively.

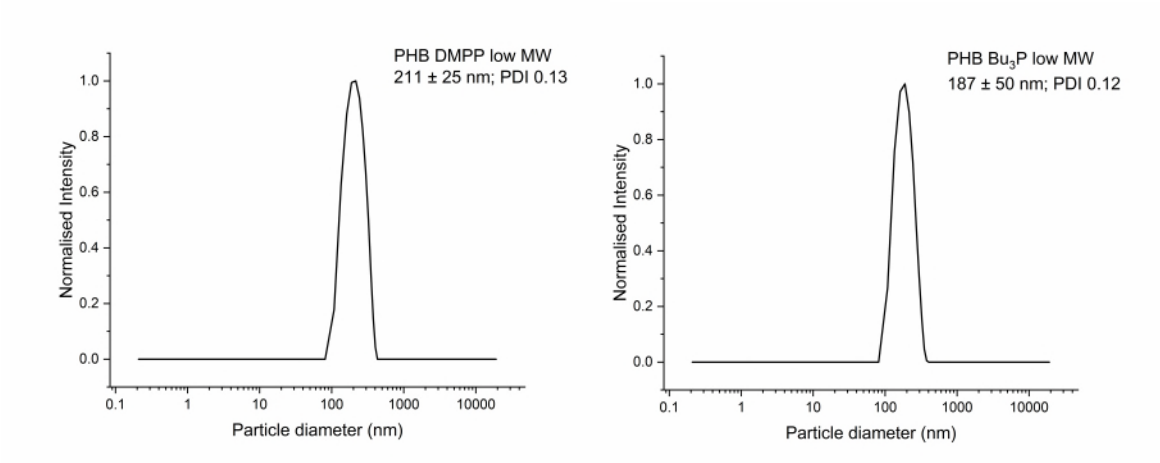

Figure S20: Intensity-weighed particle diameter measured via dynamic light scattering recorded for low molecular weight PHB functionalised with DMPP (left) and Bu_3P (right), respectively.

Thiol-ene functionalisation

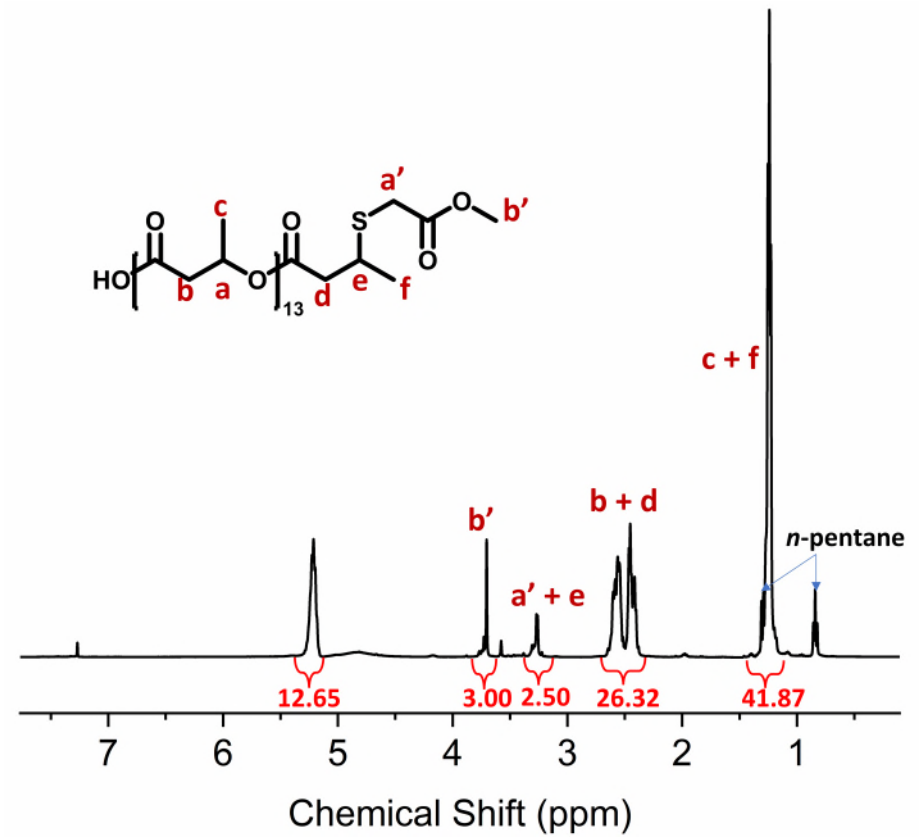

Figure S21: ^{1}H-NMR of PHB functionalised with MTG via thiol-ene click chemistry.

Medium molecular weight PHB

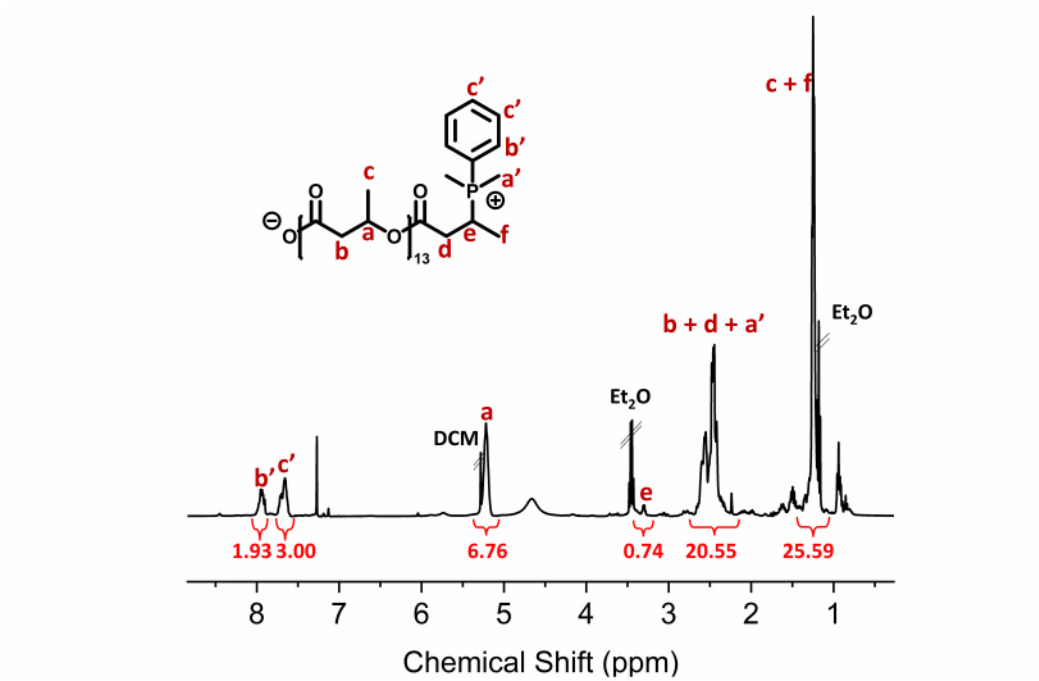

Figure S22: ^{1}H-NMR (400 MHz. $CDCl_3$) of medium molecular weight PHB functionalised with DMPP.

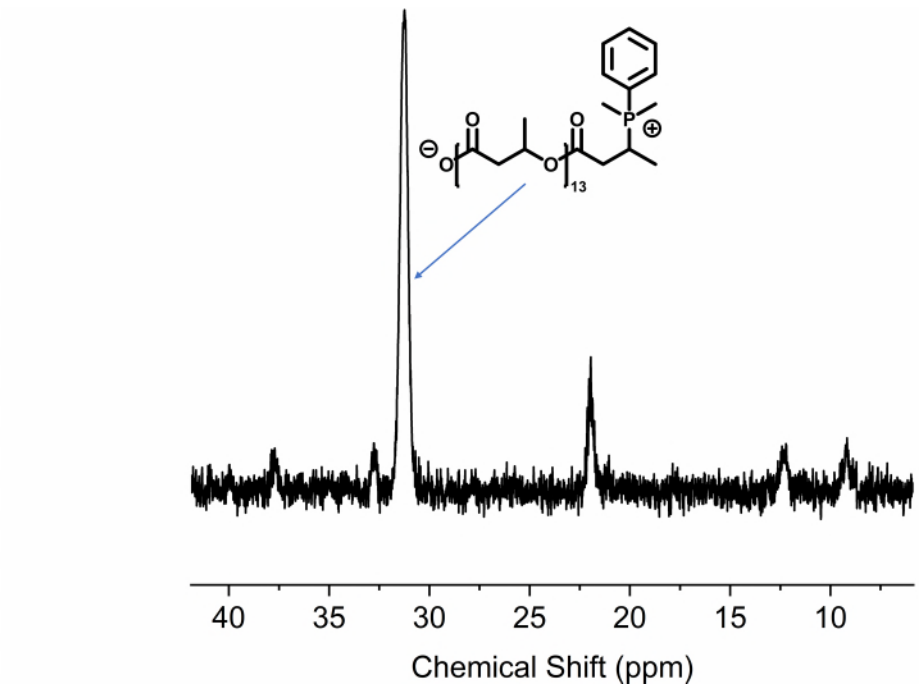

Figure S23: ^{31}P-NMR (162 MHz. $CDCl_3$) of medium molecular weight PHB functionalised with DMPP.

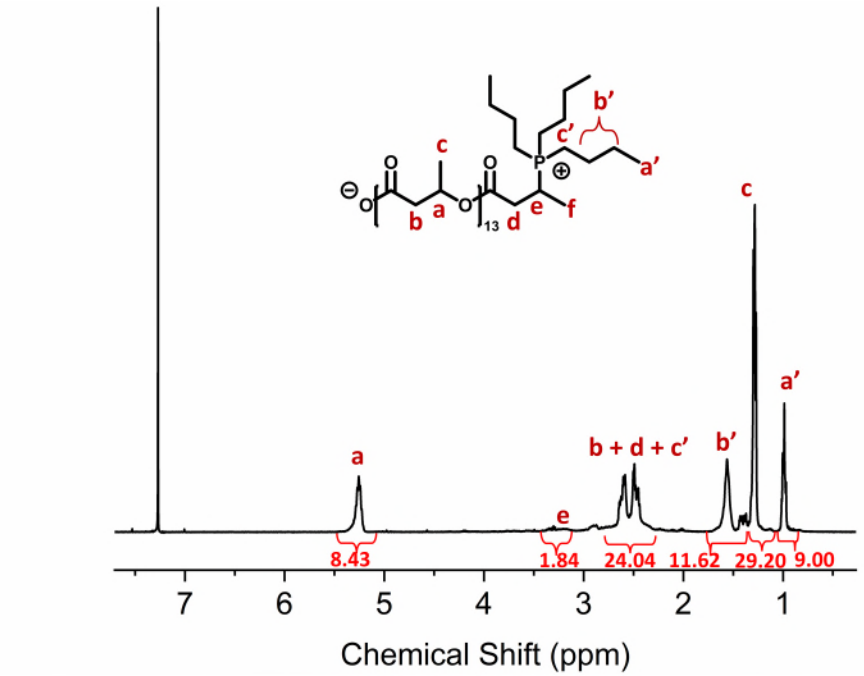

Figure S24: ^{1}H-NMR (400 MHz. $CDCl_3$) of medium molecular weight PHB functionalised with Bu_3P.

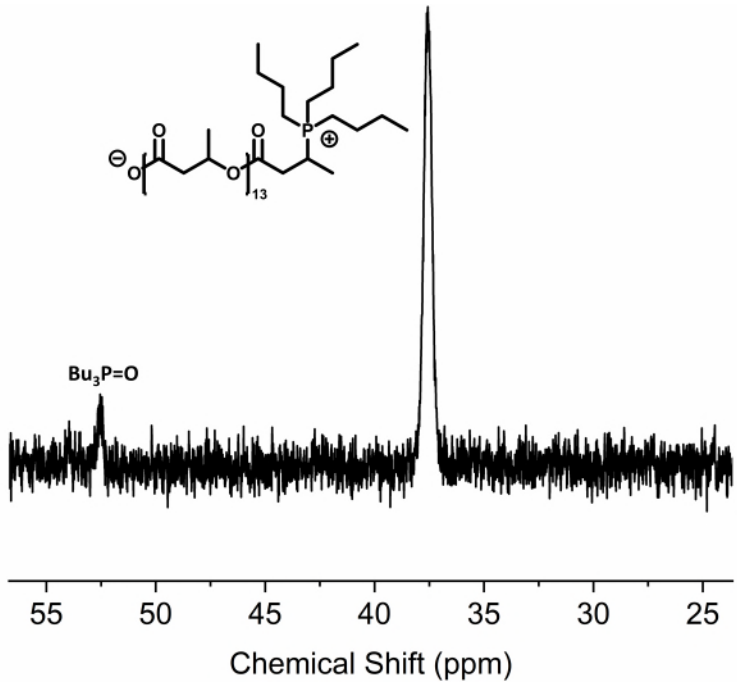

Figure S25: ^{31}P-NMR (162 MHz. $CDCl_3$) of medium molecular weight PHB functionalised with Bu_3P.

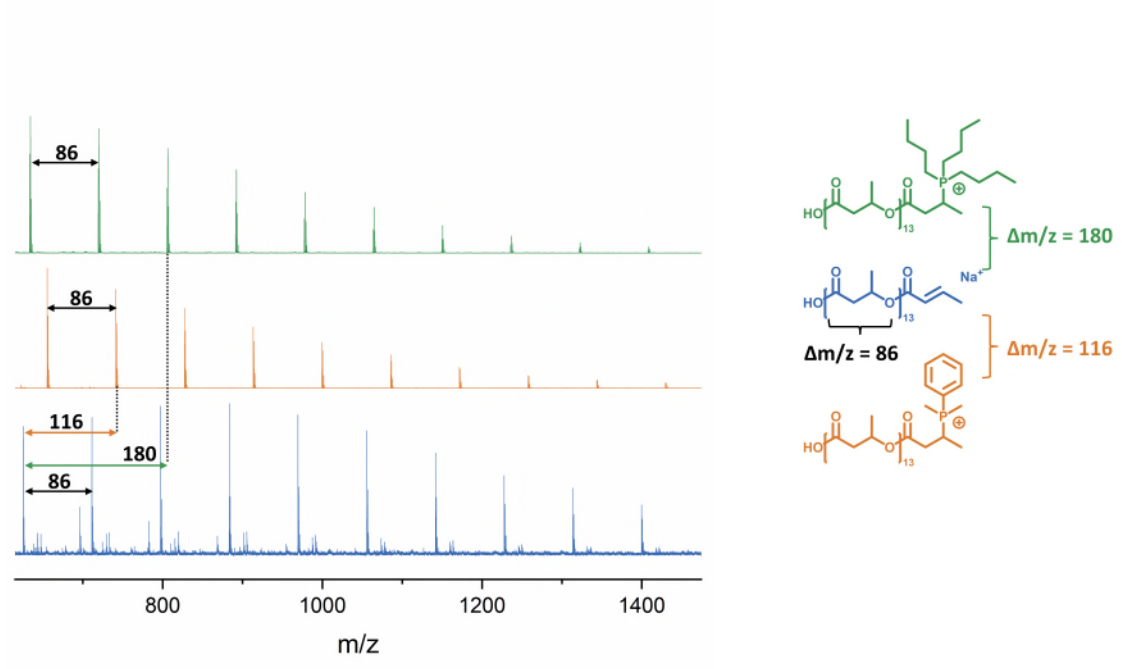

Figure S26: MALDI-ToF spectra of unfunctionalised (uf) medium molecular weight PHB compared to PHB functionalised with DMPP and Bu_3P, respectively.

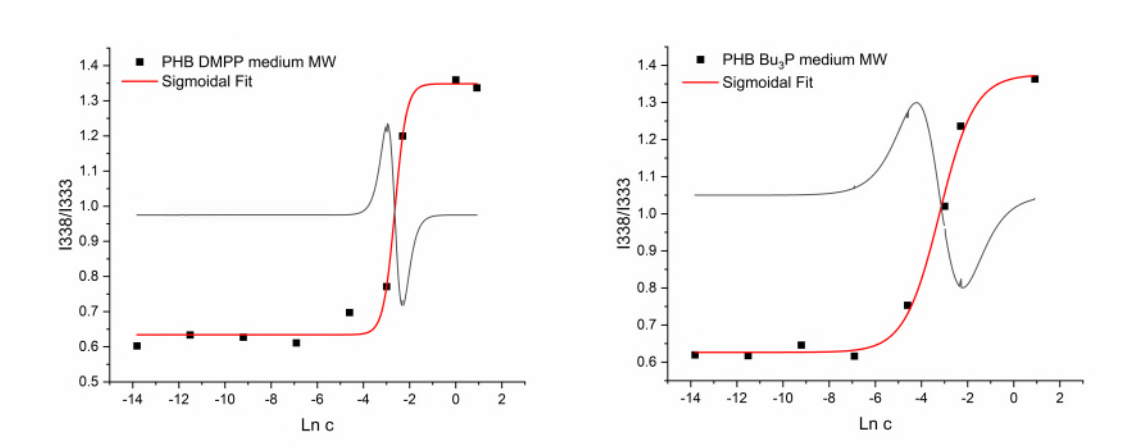

Figure S27: Plots of the relationship between fluorescence emission at 338 nm and 333 nm with a logarithmic concentration, measured for different medium molecular weight polymer adduct concentrations in the presence of pyrene. PHB DMPP (left), PHB Bu_3P (right).

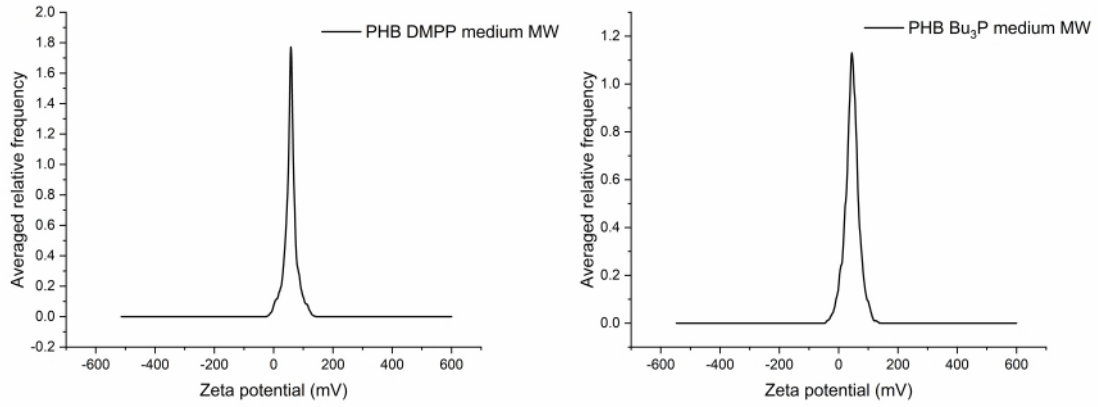

Figure S28: Zeta potential recorded for medium molecular weight PHB functionalised with DMPP (left) and Bu_3P (right), respectively.

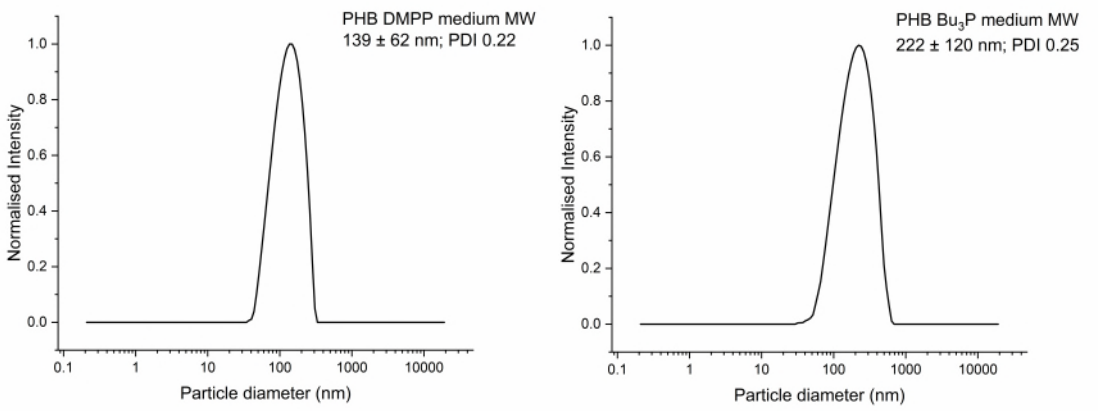

Figure S29: Intensity-weighed particle diameter measured via dynamic light scattering recorded for medium molecular weight PHB functionalised with DMPP (left) and Bu_3P (right), respectively.

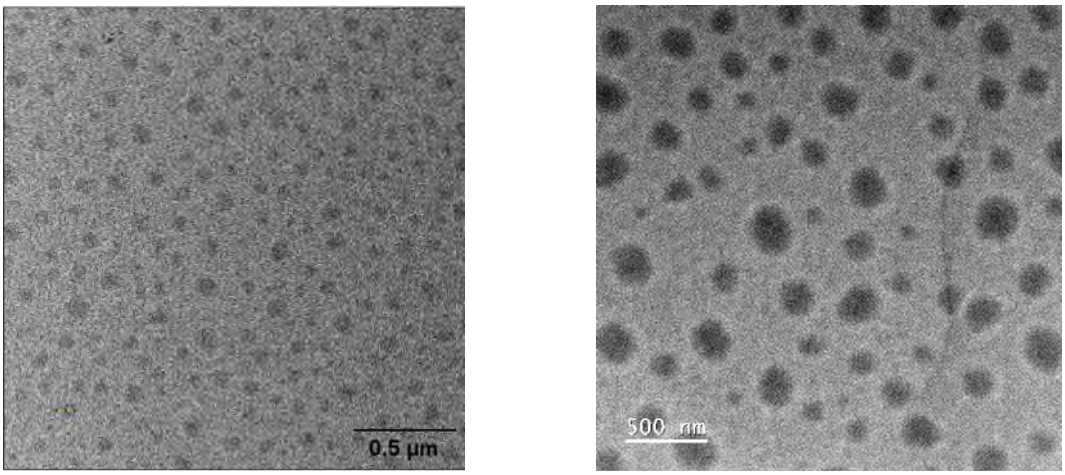

Figure S30: TEM pictures taken for medium molecular weight PHB, functionalised with DMPP (left) and Bu_3P (right), respectively. Samples were prepared by drying aqueous polymer suspensions.

Medium high molecular weight PHB

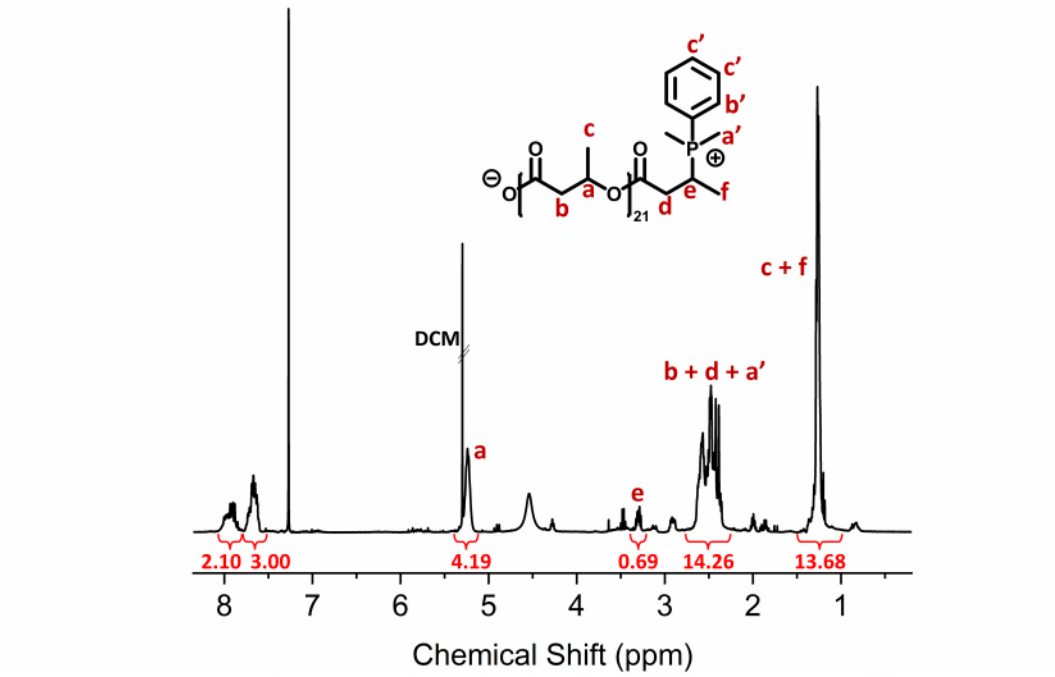

Figure S31: ^{1}H-NMR (400 MHz. $CDCl_3$) of medium high molecular weight PHB functionalised with DMPP.

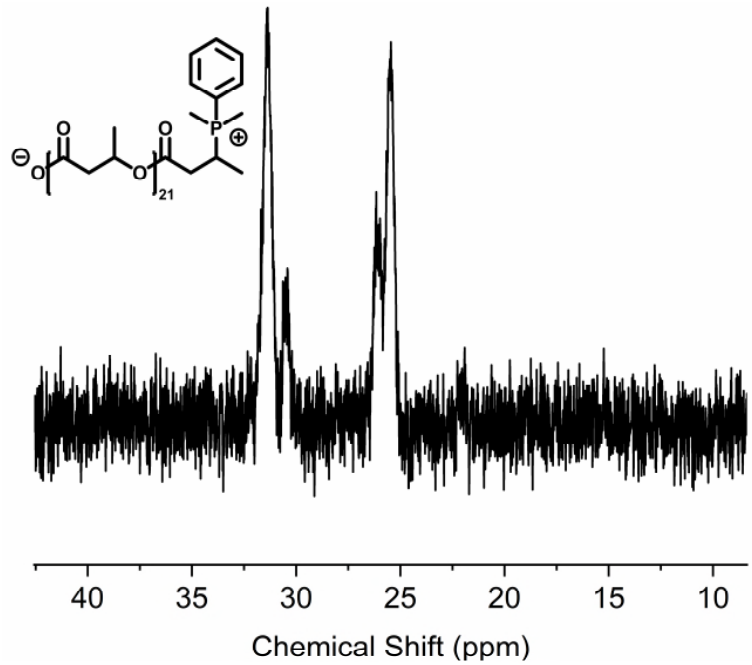

Figure S32: ^{31}P-NMR (162 MHz. $CDCl_3$) of medium high molecular weight PHB functionalised with DMPP.

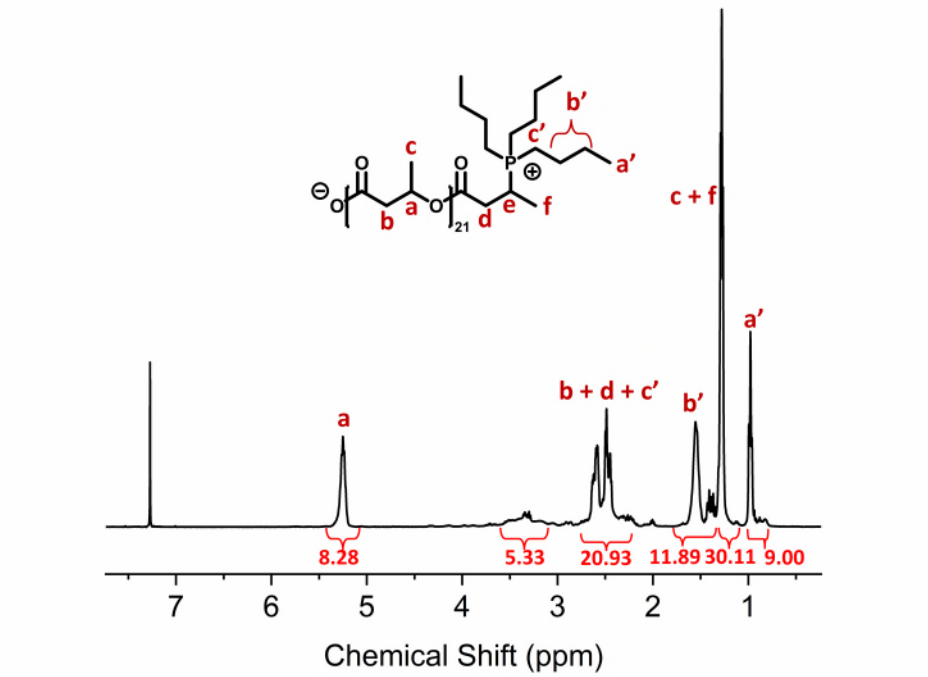

Figure S33: ^{1}H-NMR (400 MHz. $CDCl_3$) of medium high molecular weight PHB functionalised with Bu_3P.

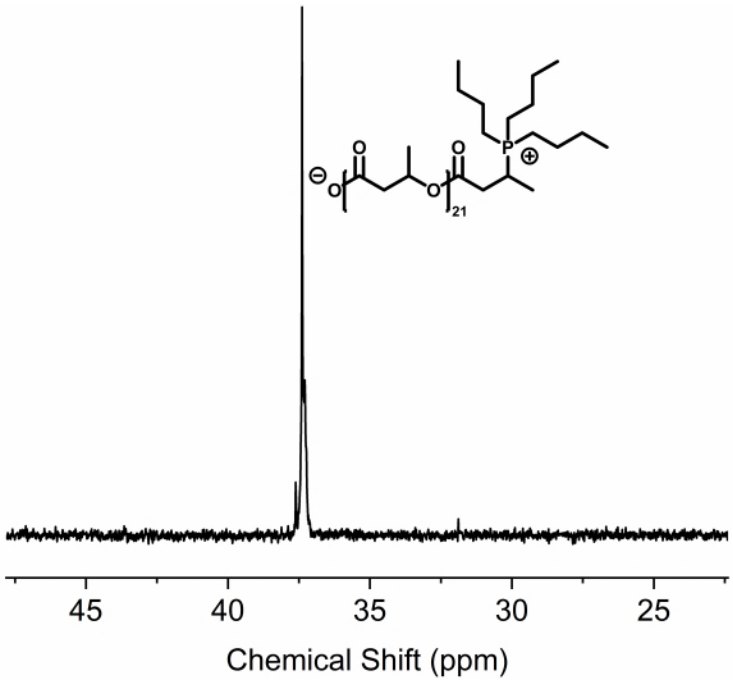

Figure S34: ^{31}P-NMR (162 MHz. $CDCl_3$) of medium high molecular weight PHB functionalised with Bu_3P.

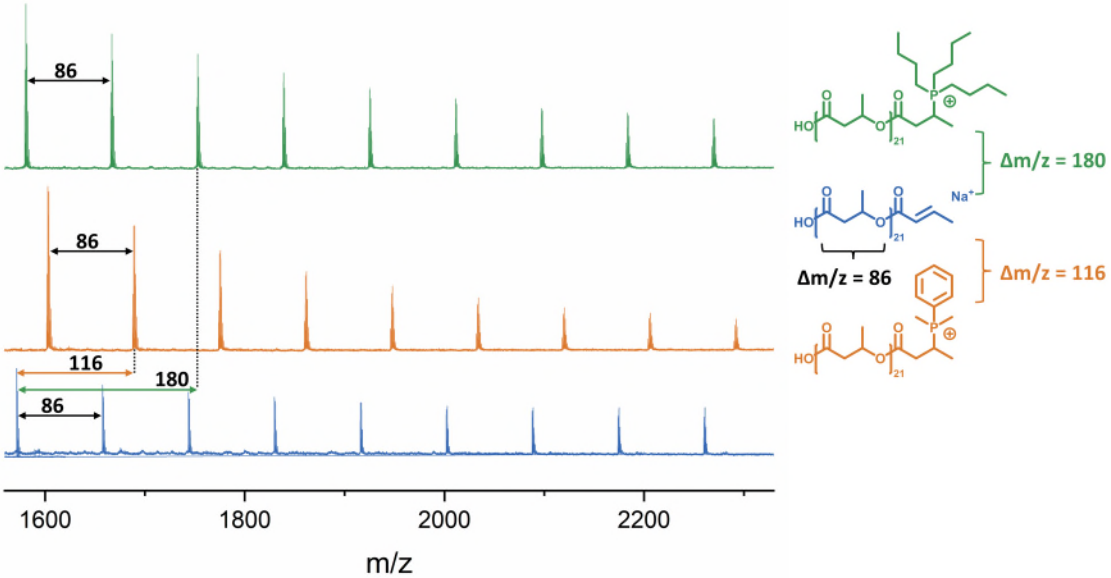

Figure S35: MALDI-ToF spectra of unfunctionalised (uf) medium high molecular weight PHB compared to PHB functionalised with DMPP and Bu_3P, respectively.

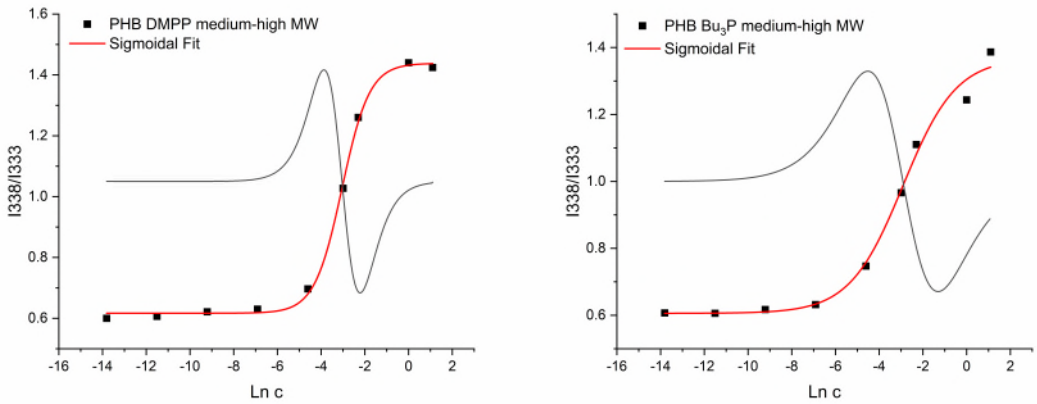

Figure S36: Plots of the relationship between fluorescence emission at 338 nm and 333 nm with a logarithmic concentration, measured for different medium high molecular weight polymer adduct concentrations in the presence of pyrene. PHB DMPP (left), PHB Bu_3P (right).

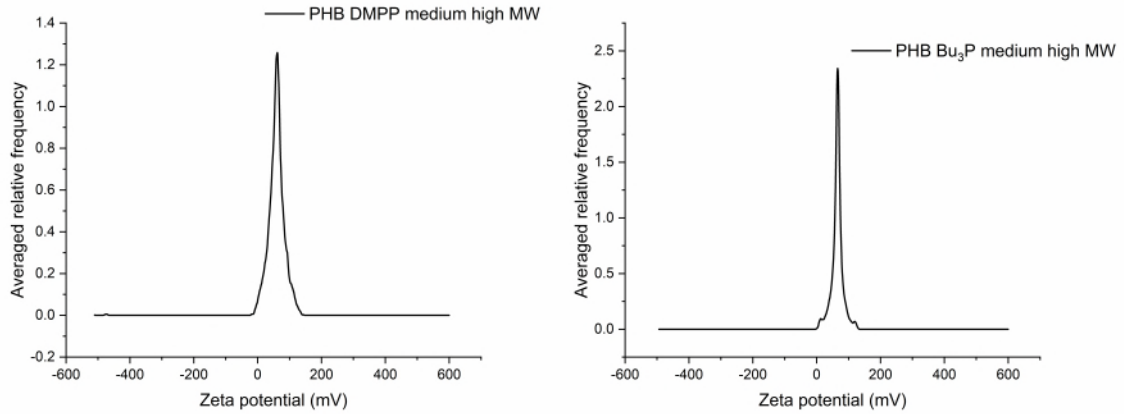

Figure S37: Zeta potential recorded for medium high molecular weight PHB functionalised with DMPP (left) and Bu_3P (right), respectively.

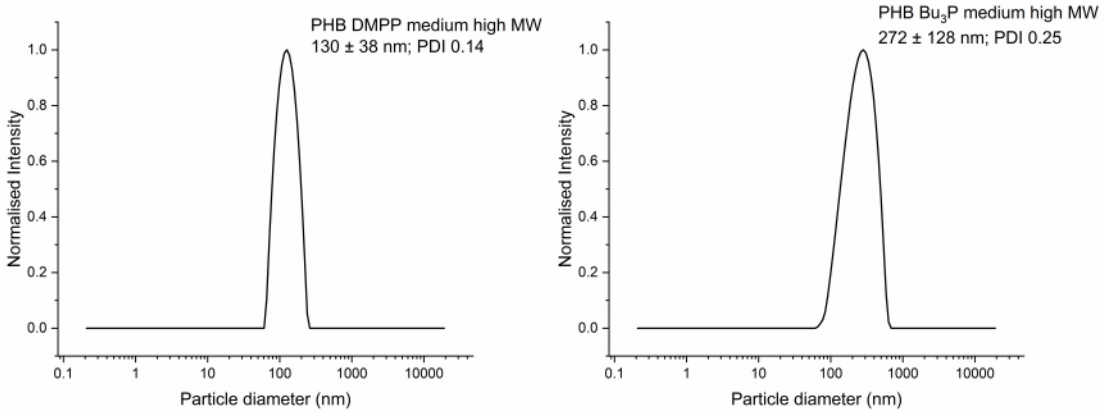

Figure S38: Intensity-weighed particle diameter measured via dynamic light scattering recorded for medium high molecular weight PHB functionalised with DMPP (left) and Bu_3P (right), respectively.

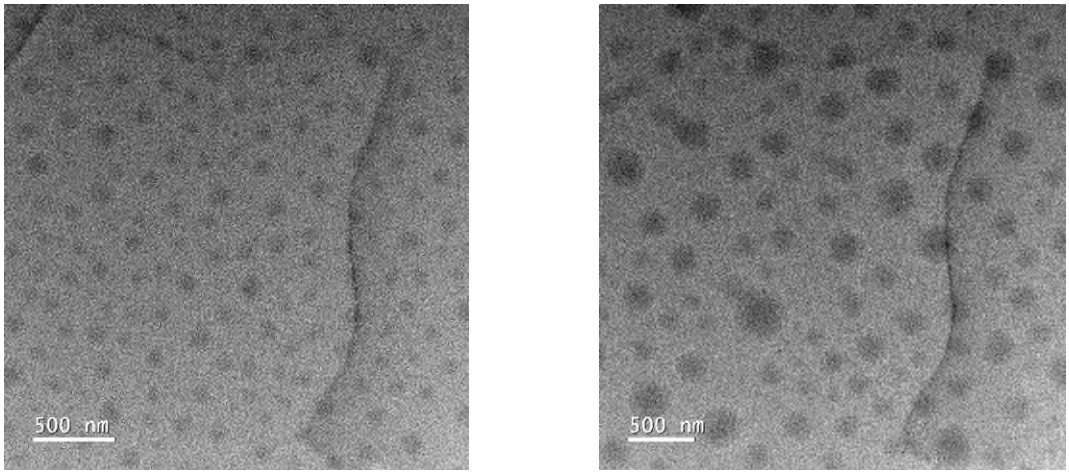

Figure S39: TEM pictures taken for medium high molecular weight PHB, functionalised with DMPP (left) and Bu_3P (right), respectively. Samples were prepared by drying aqueous polymer suspensions.

High molecular weight PHB

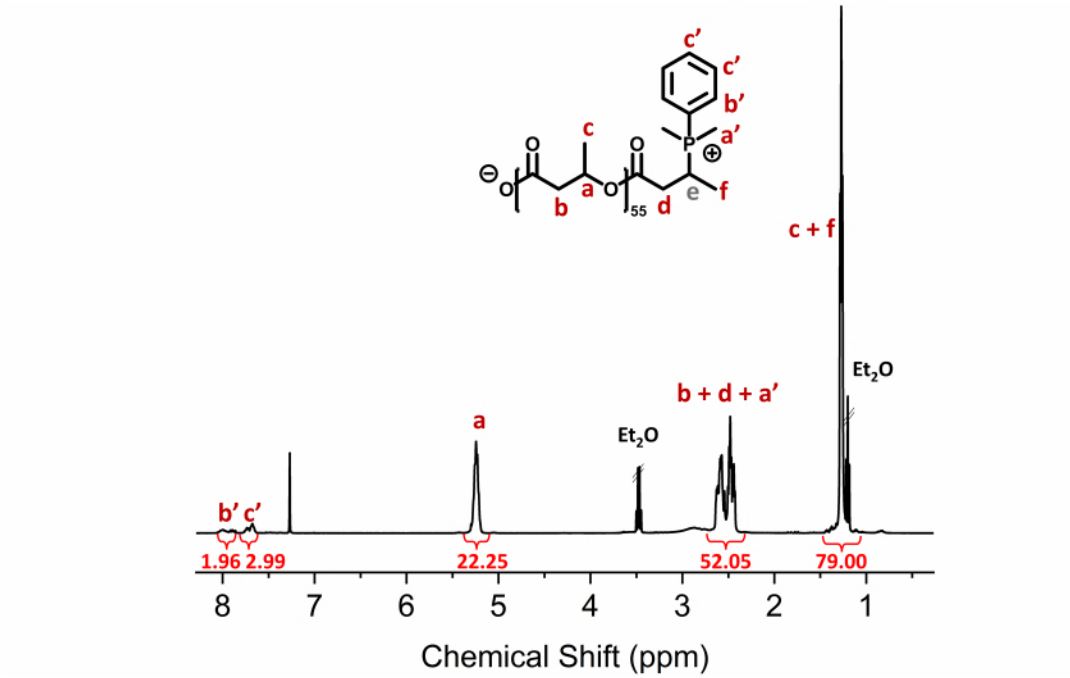

Figure S40: ^{1}H-NMR (400 MHz. $CDCl_3$) of high molecular weight PHB functionalised with DMPP.

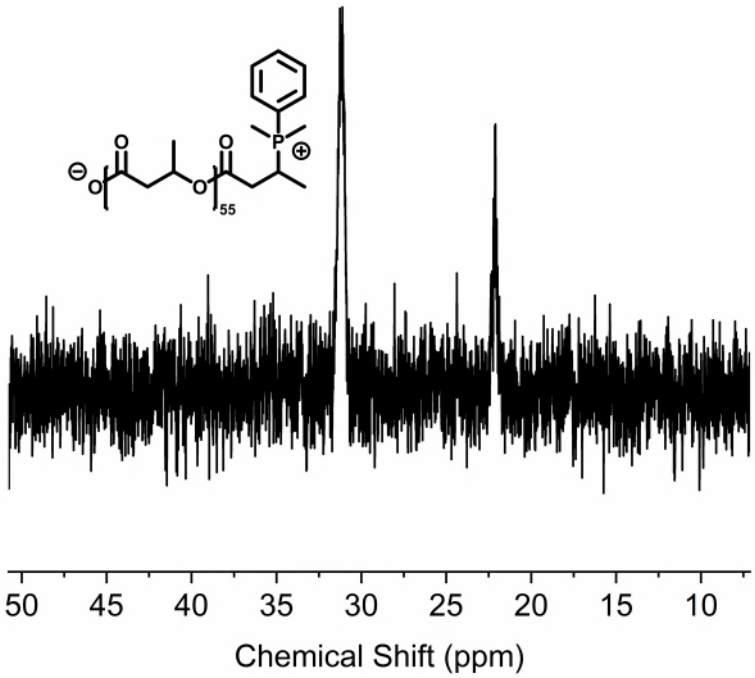

Figure S41: ^{31}P-NMR (162 MHz. $CDCl_3$) of high molecular weight PHB functionalised with DMPP.

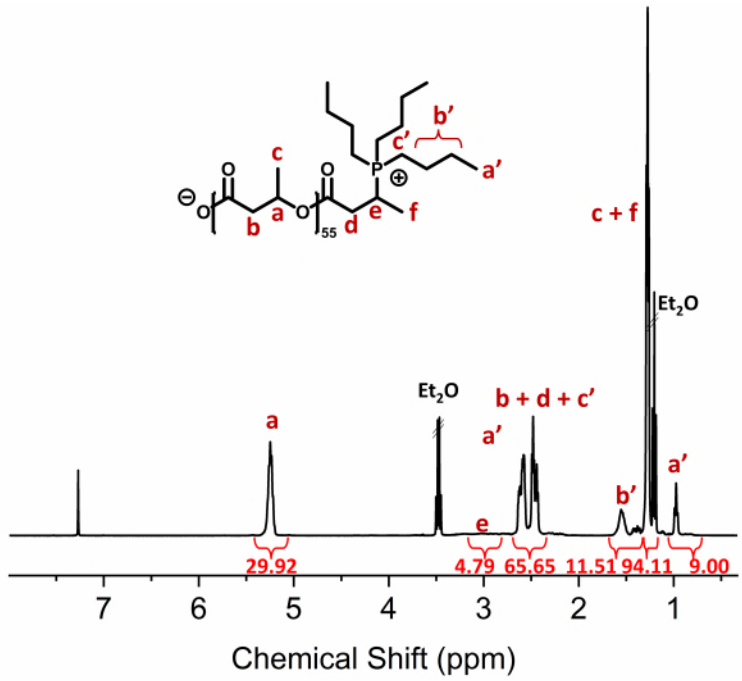

Figure S42: ^{1}H-NMR (400 MHz. $CDCl_3$) of high molecular weight PHB functionalised with Bu_3P.

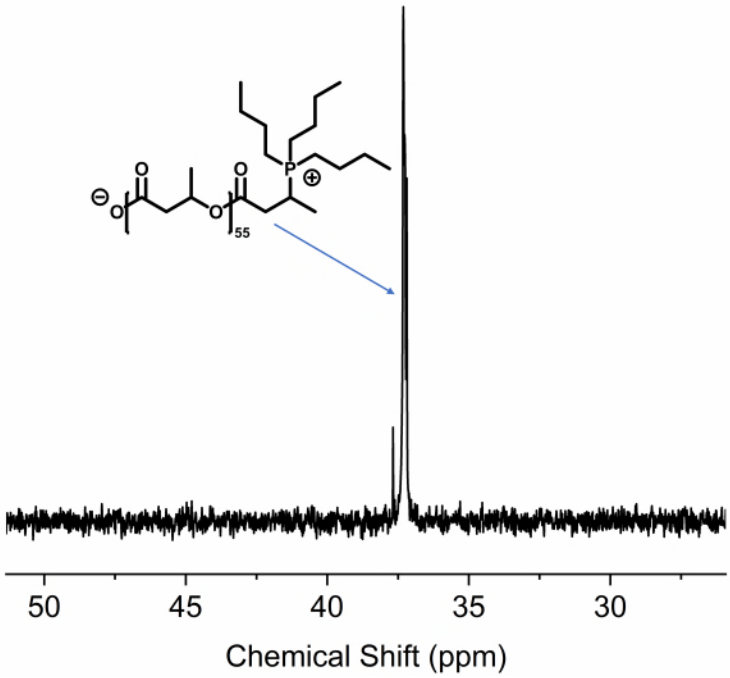

Figure S43: ^{31}P-NMR (162 MHz. $CDCl_3$) of high molecular weight PHB functionalised with Bu_3P.

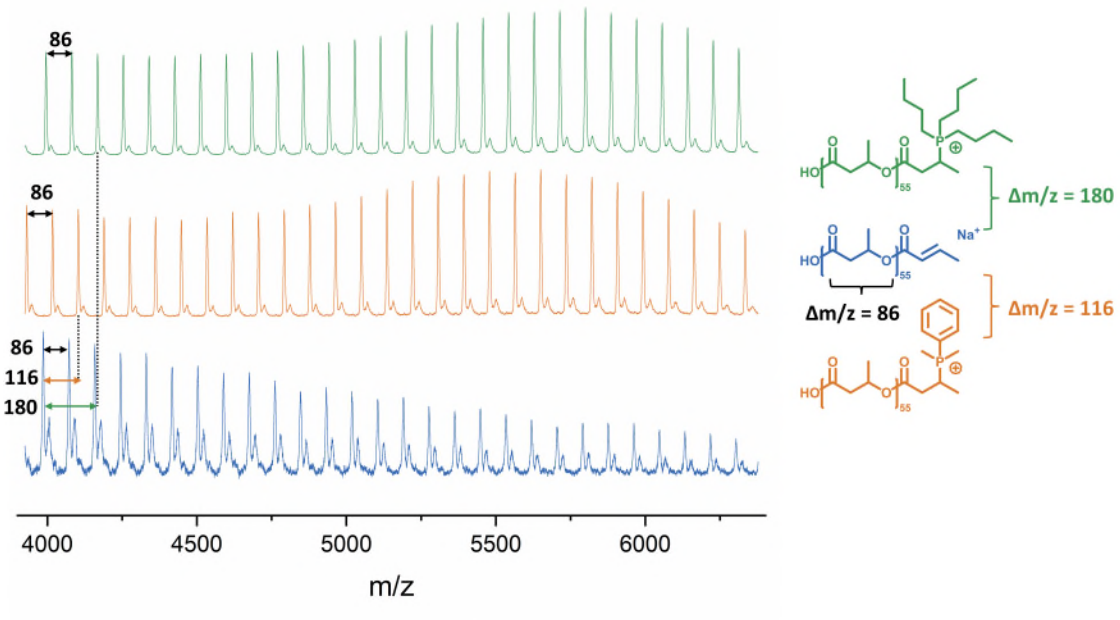

Figure S44: MALDI-ToF spectra of unfunctionalised (uf) high molecular weight PHB compared to PHB functionalised with DMPP and Bu_3P, respectively. All spectra have been measured in linear mode.

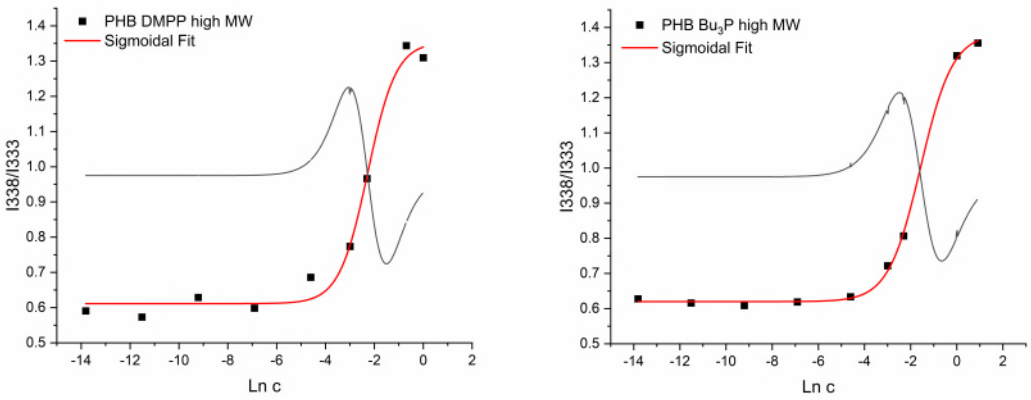

Figure S45: Plots of the relationship between fluorescence emission at 338 nm and 333 nm with a logarithmic concentration, measured for different high molecular weight polymer adduct concentrations in the presence of pyrene. PHB DMPP (left), PHB Bu_3P (right).

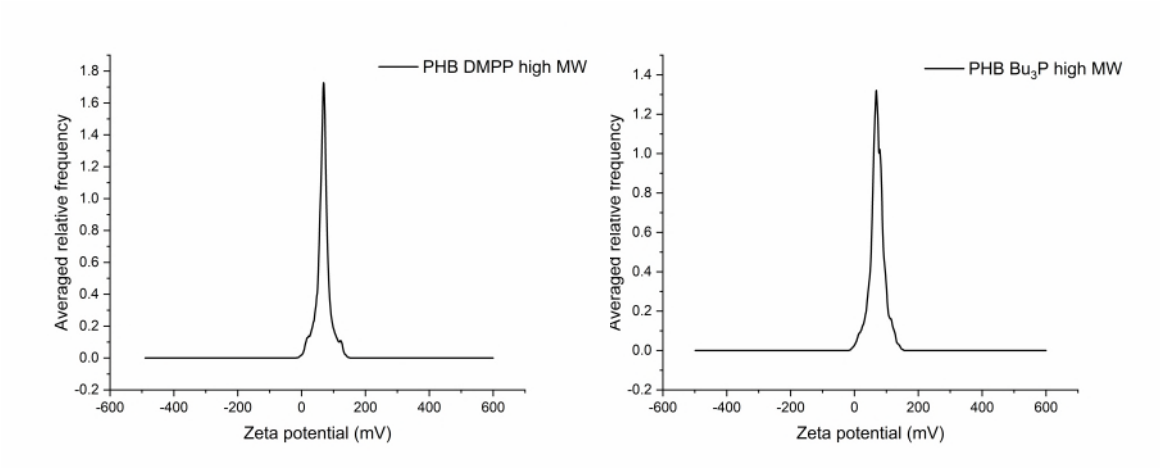

Figure S46: Zeta potential recorded for high molecular weight PHB functionalised with DMPP (left) and Bu_3P (right), respectively.

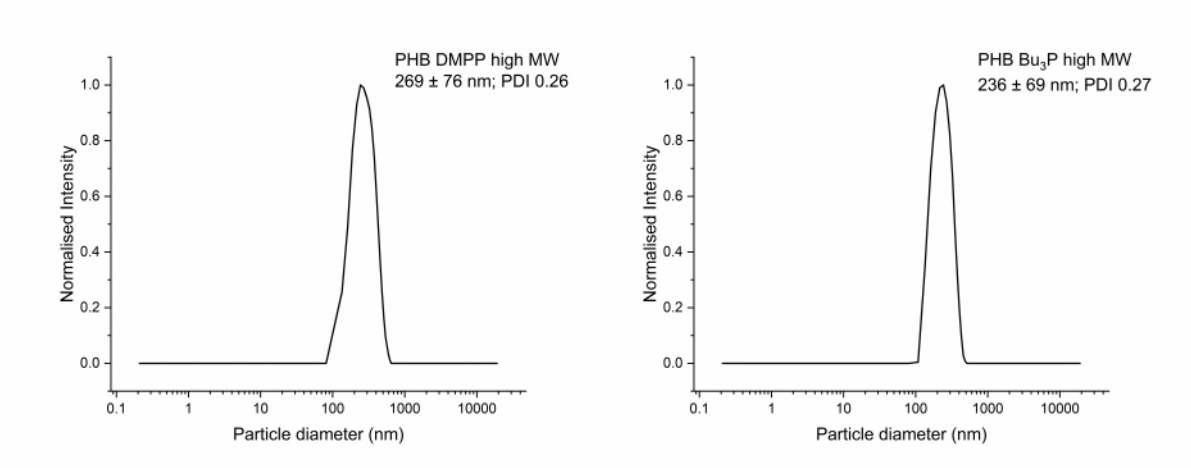

Figure S47: Intensity-weighed particle diameter measured via dynamic light scattering recorded for high molecular weight PHB functionalised with DMPP (left) and Bu_3P (right), respectively.

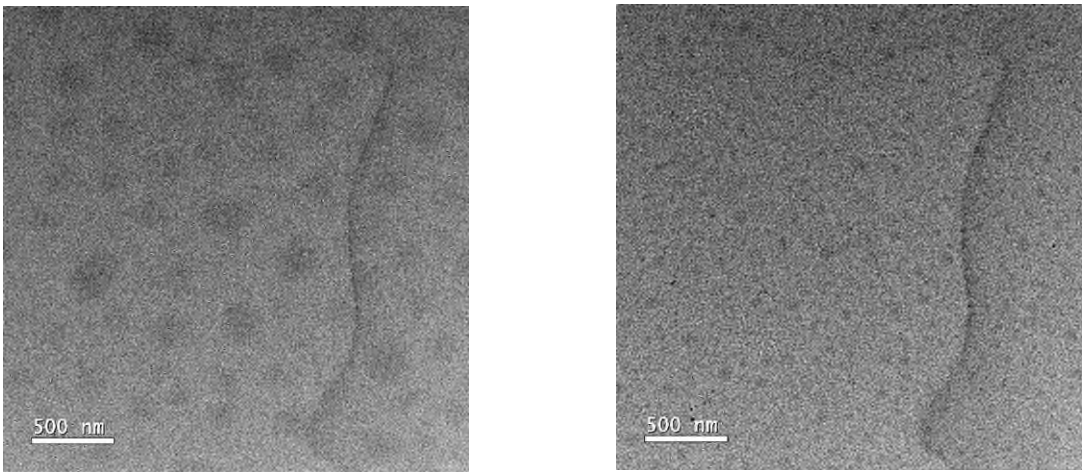

Figure S48: TEM pictures taken for high molecular weight PHB, functionalised with DMPP (left) and Bu_3P (right), respectively. Samples were prepared by drying aqueous polymer suspensions.

1.4 Control experiments on small molecules

1.4.1 Crotonic acid and DMPP

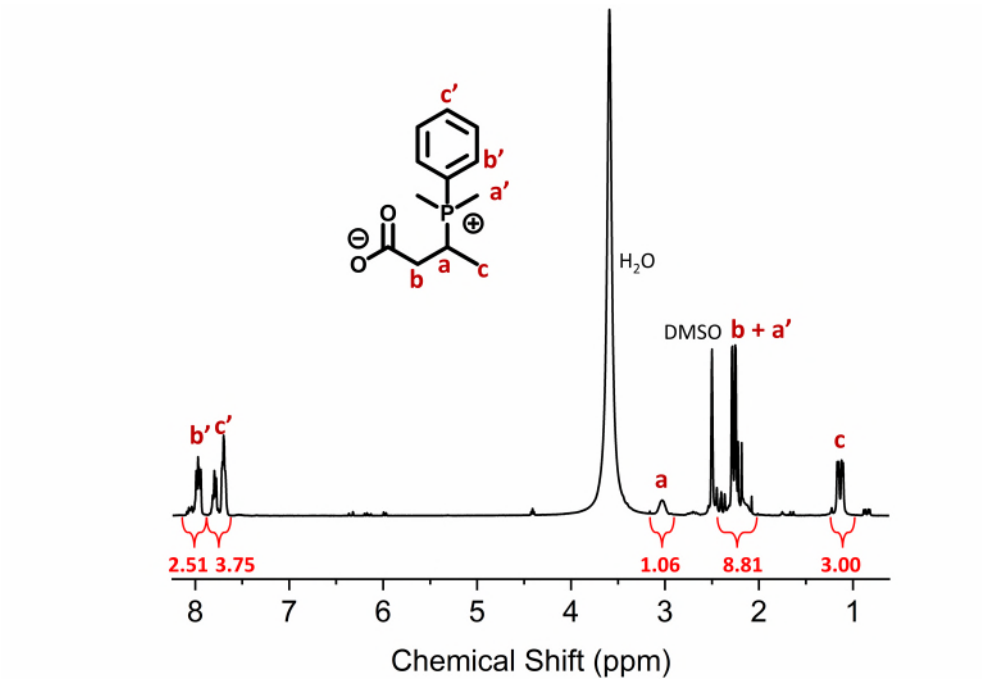

Figure S49: ^{1}H-NMR (400 MHz, DMSO-d^{6}) of crotonic acid functionalised with DMPP.

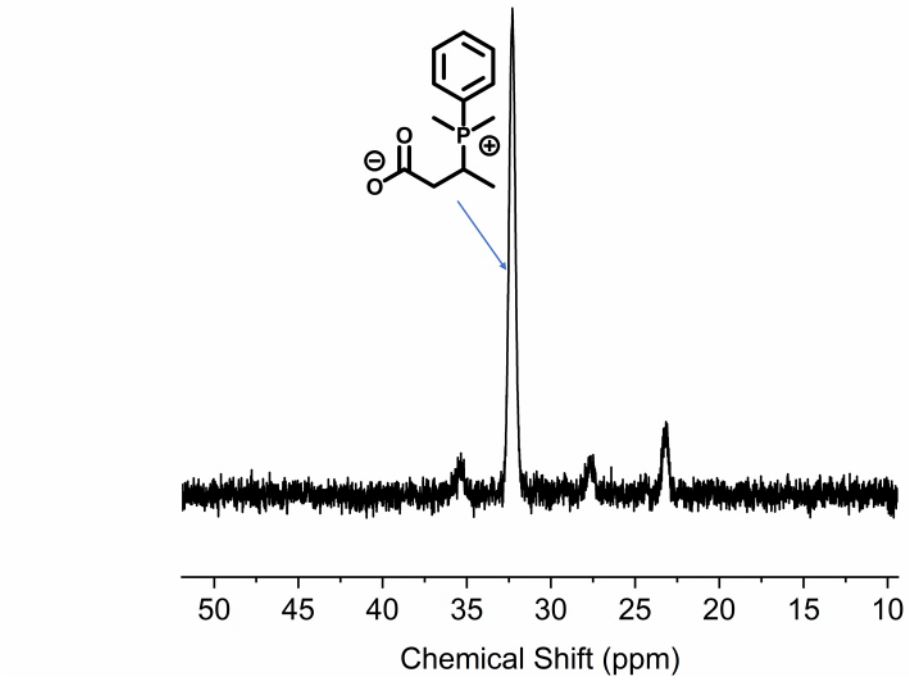

Figure S50: ^{31}P-NMR (162 MHz, DMSO-d^{6}) of crotonic acid functionalised with DMPP.

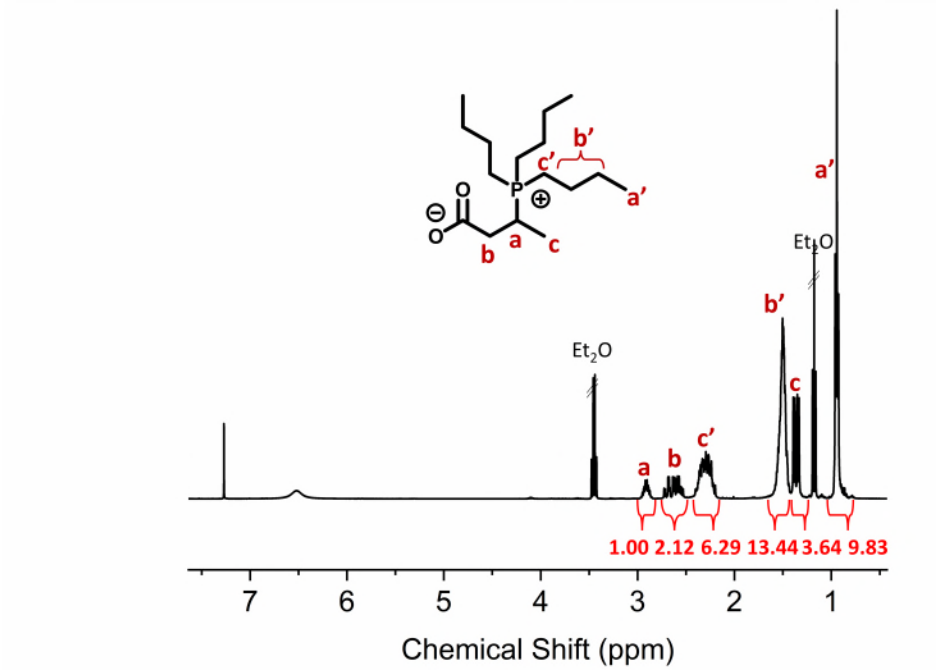

Figure S51: ^{1}H-NMR (400 MHz, $CDCl_3$) of crotonic acid functionalised with Bu_3P.

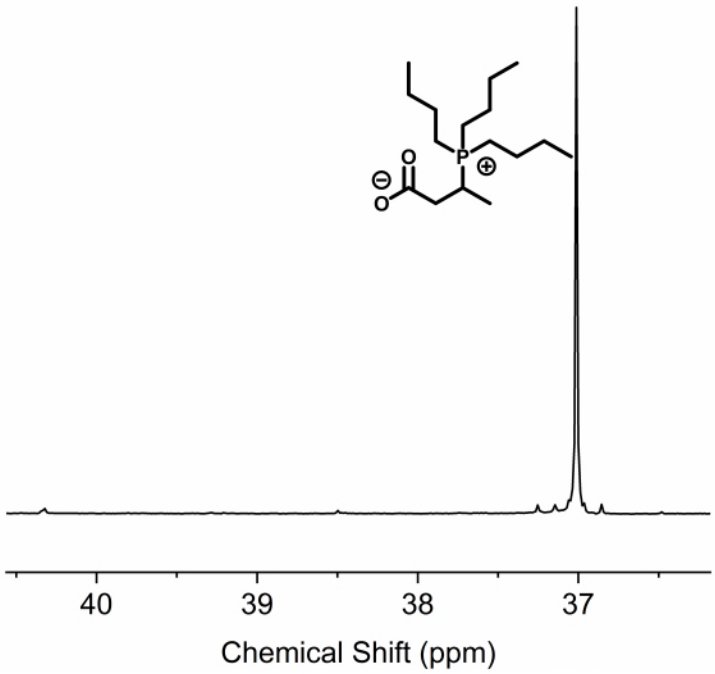

Figure S52: ^{31}P-NMR (162 MHz, DMSO-d^{6}) of crotonic acid functionalised with Bu_3P.

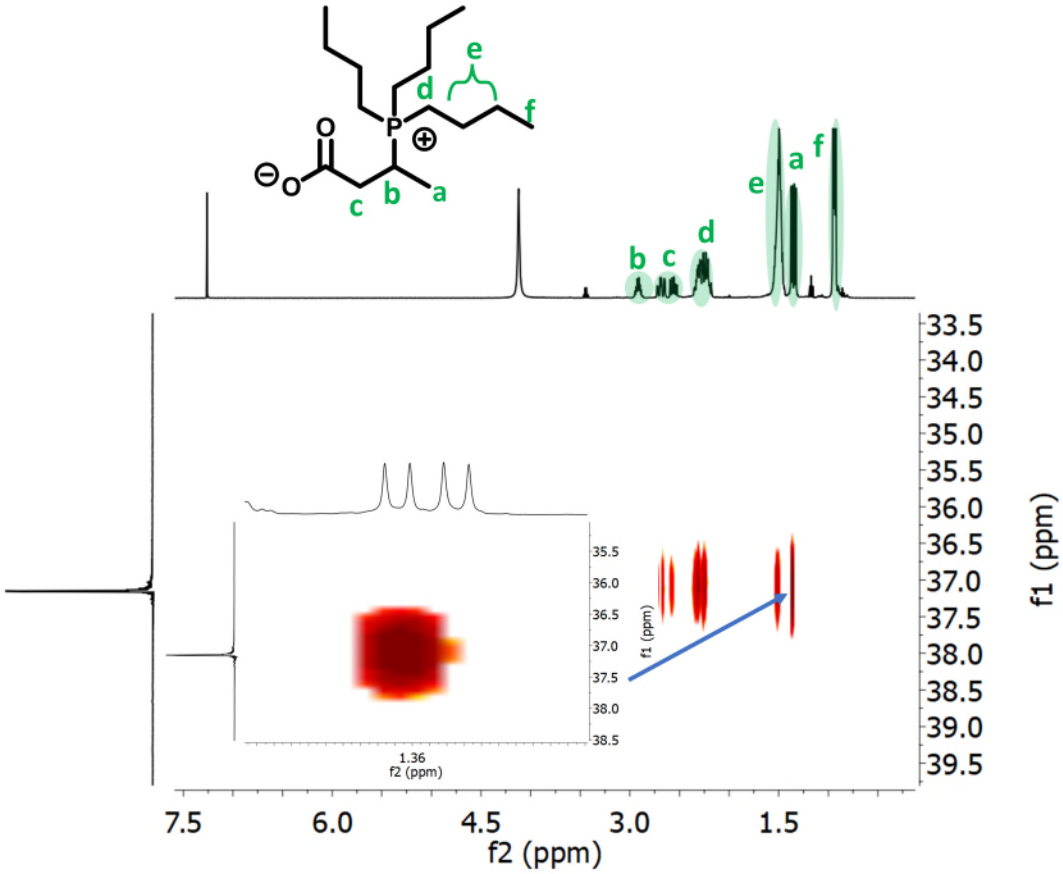

Figure S53: ^{1}H-^{31}P correlation NMR (500 MHz ^{1}H; 200 MHz ^{31}P. $CDCl_3$) of crotonic acid functionalised with Bu_3P.

1.4.2 Methyl crotonate/*n*-butyric acid and DMPP

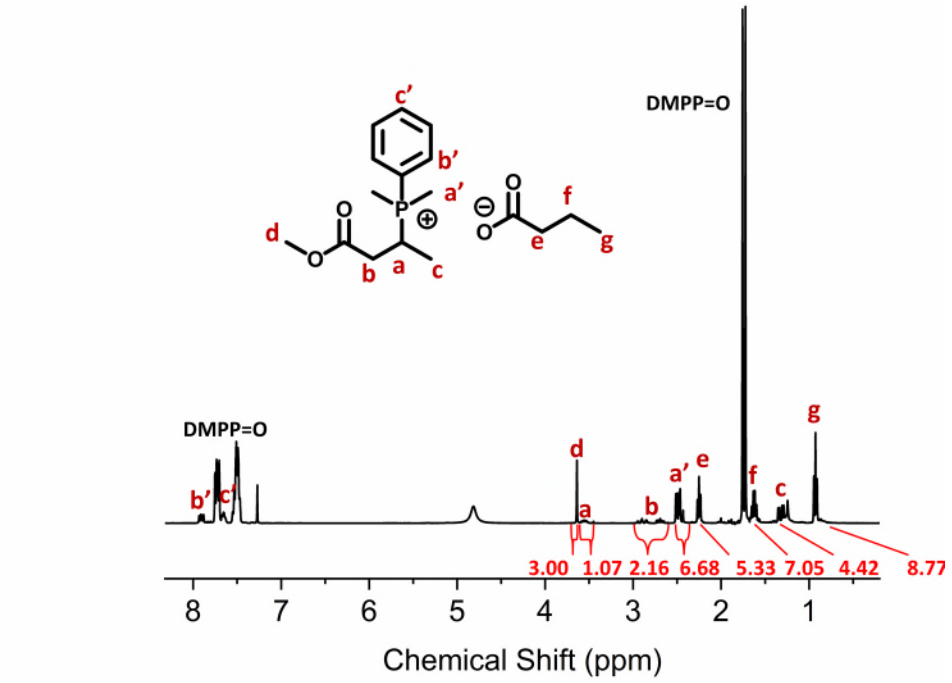

Figure S54: ^{1}H-NMR (400 MHz. $CDCl_3$) of Methyl-crotonate functionalised with DMPP and *n*-butyric acid.

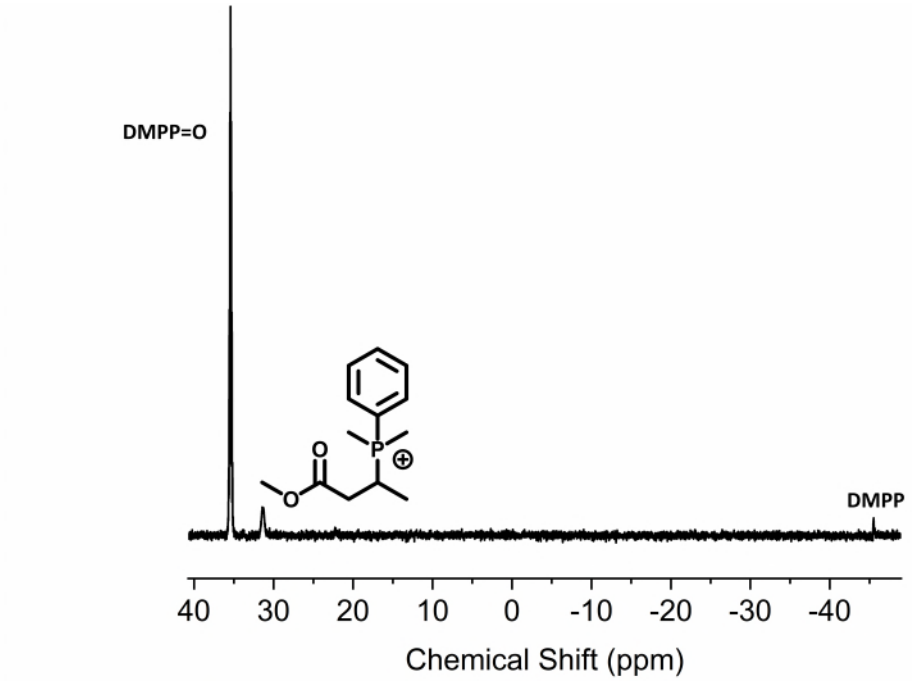

Figure S55: ^{31}P-NMR (162 MHz. $CDCl_3$) of Methyl-crotonate functionalised with DMPP.

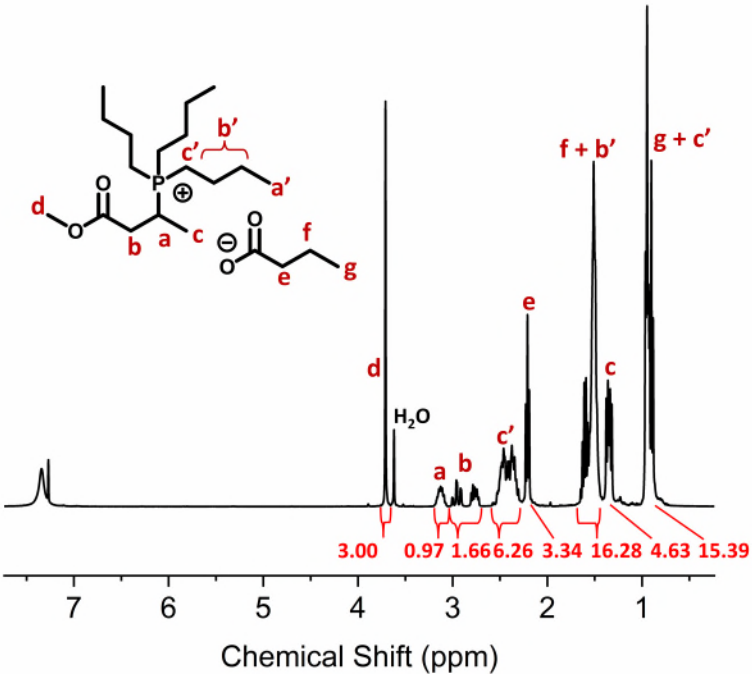

Figure S56: ^{1}H-NMR (400 MHz. $CDCl_3$) of Methyl-crotonate functionalised with Bu_3P and *n*-butyric acid.

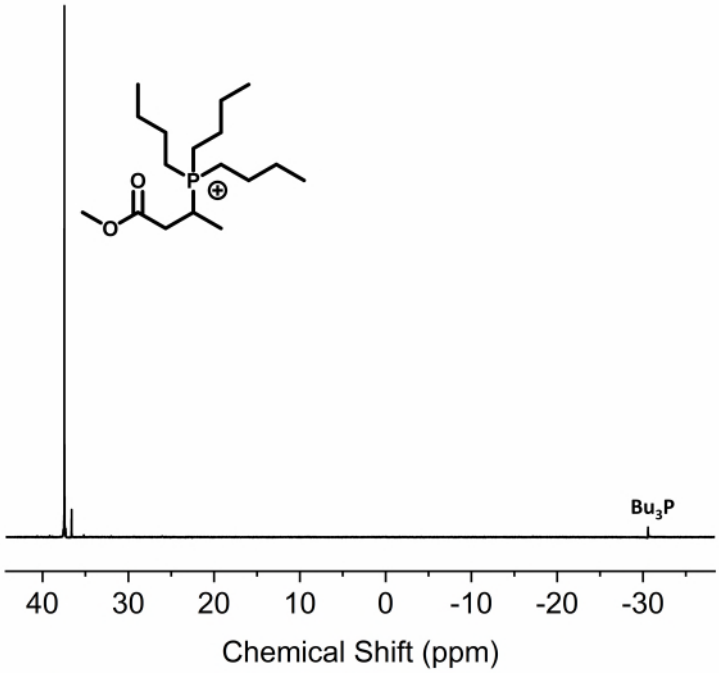

Figure S57: ^{31}P-NMR (162 MHz. $CDCl_3$) of Methyl-crotonate functionalised with Bu_3P.

1.4.3 Self-assembly as a function of salt and pH

NaCl

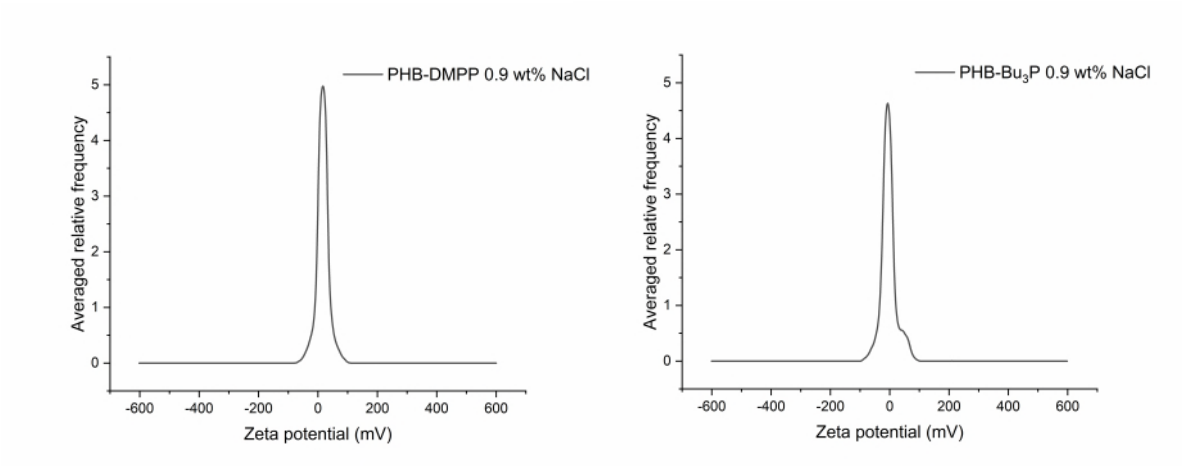

Figure S58:Zeta potential recorded for low molecular weight functionalised PHB measured in 0.9 wt% NaCl solution.

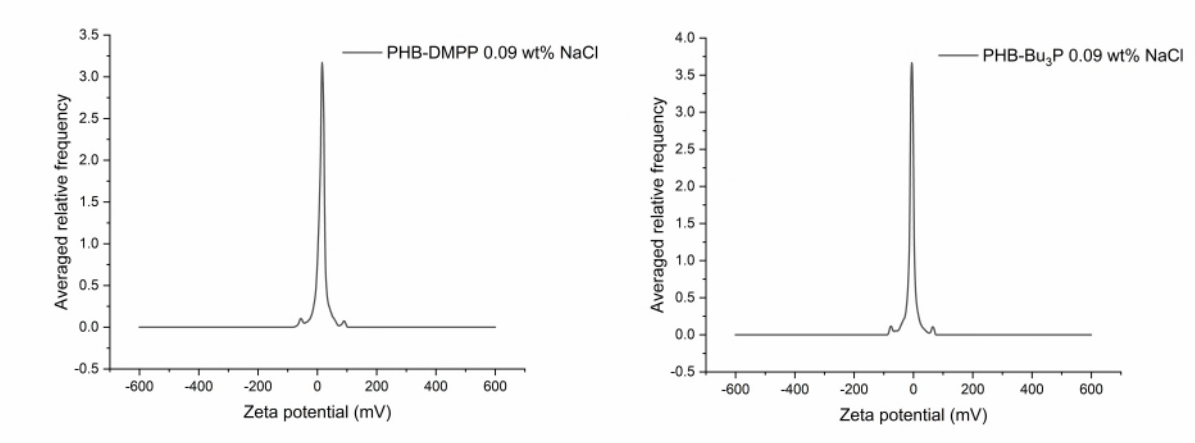

Figure S59:Zeta potential recorded for low molecular weight functionalised PHB measured in 0.09 wt% NaCl solution.

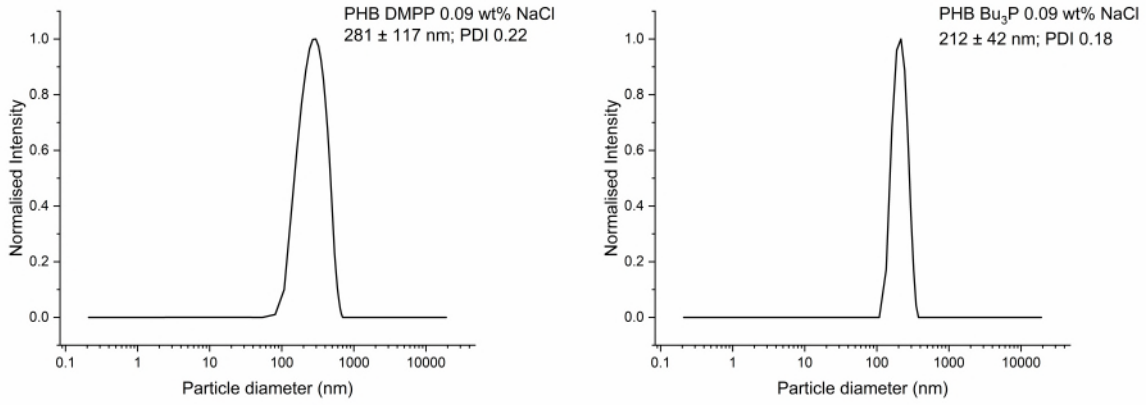

Figure S60: DLS recorded for low molecular weight functionalised PHB measured in 0.09 wt% NaCl solution.

pH 4

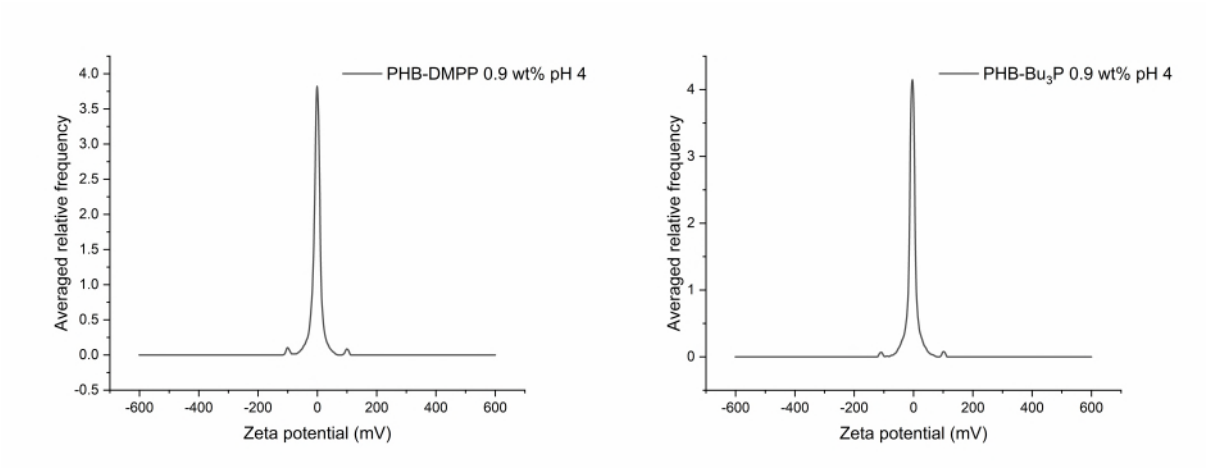

Figure S61: Zeta potential recorded for low molecular weight functionalised PHB measured in pH 4 0.9 wt% buffer solution.

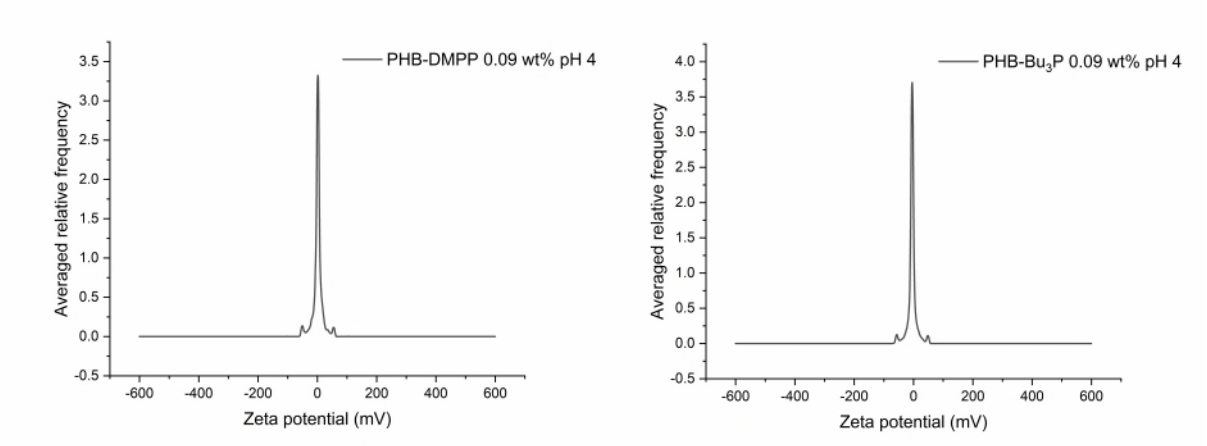

Figure S62: Zeta potential recorded for low molecular weight functionalised PHB measured in pH 4 0.09 wt% buffer solution.

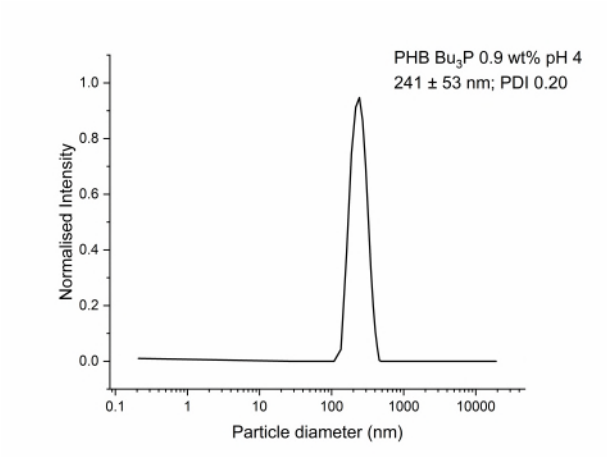

Figure S63:DLS recorded for low molecular weight functionalised PHB-Bu_3P measured in pH 4 0.9 wt% buffer solution.

pH 7

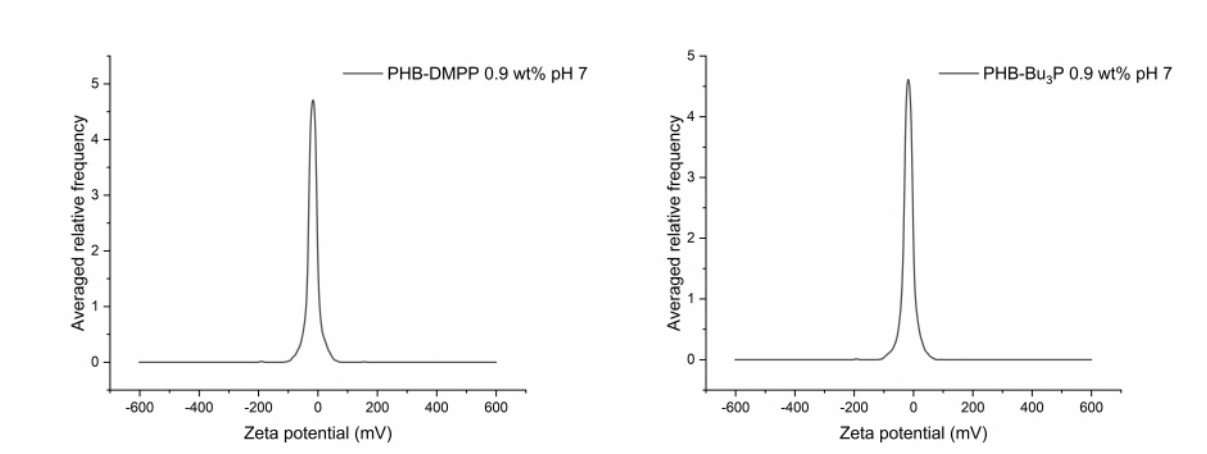

Figure S64:Zeta potential recorded for low molecular weight functionalised PHB measured in pH 7 0.9 wt% buffer solution.

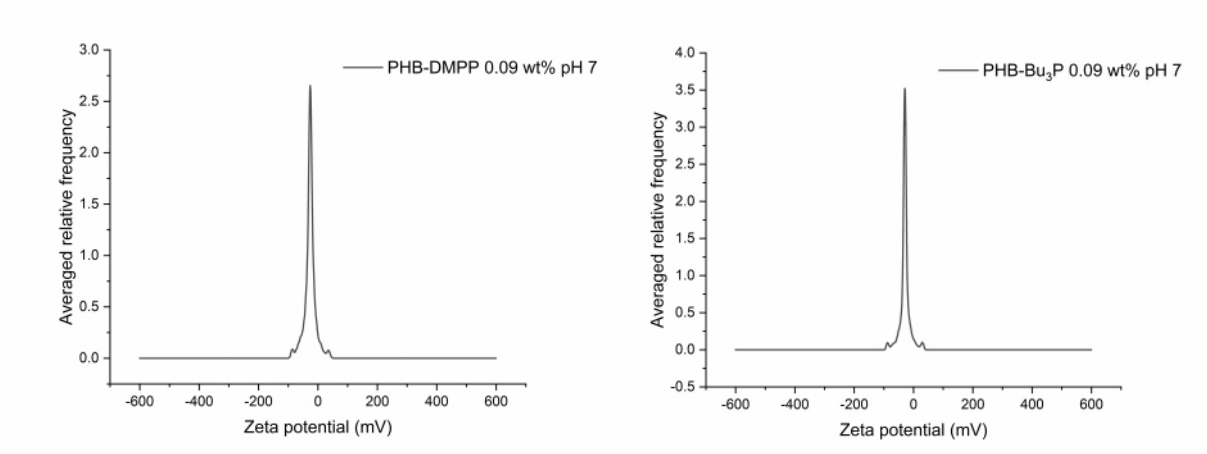

Figure S65: Zeta potential recorded for low molecular weight functionalised PHB measured in pH 7 0.09 wt% buffer solution.

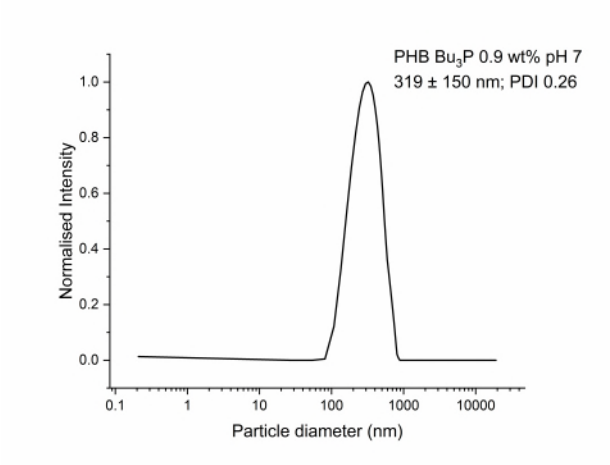

Figure S66:DLS recorded for low molecular weight functionalised PHB Bu_3P measured in pH 7 0.9 wt% buffer solution.

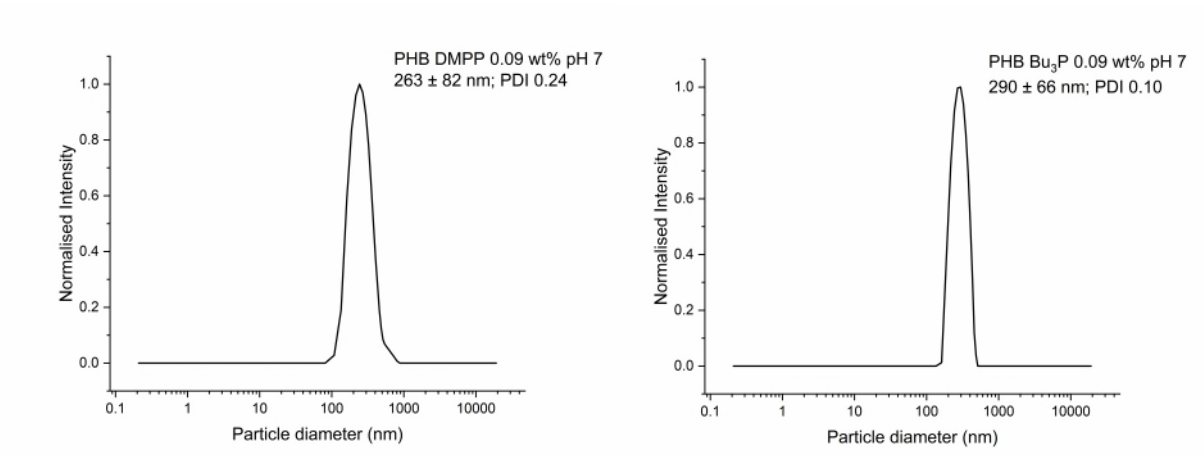

Figure S67:DLS recorded for low molecular weight functionalised PHB measured in pH 7 0.09 wt% buffer solution.

pH 9

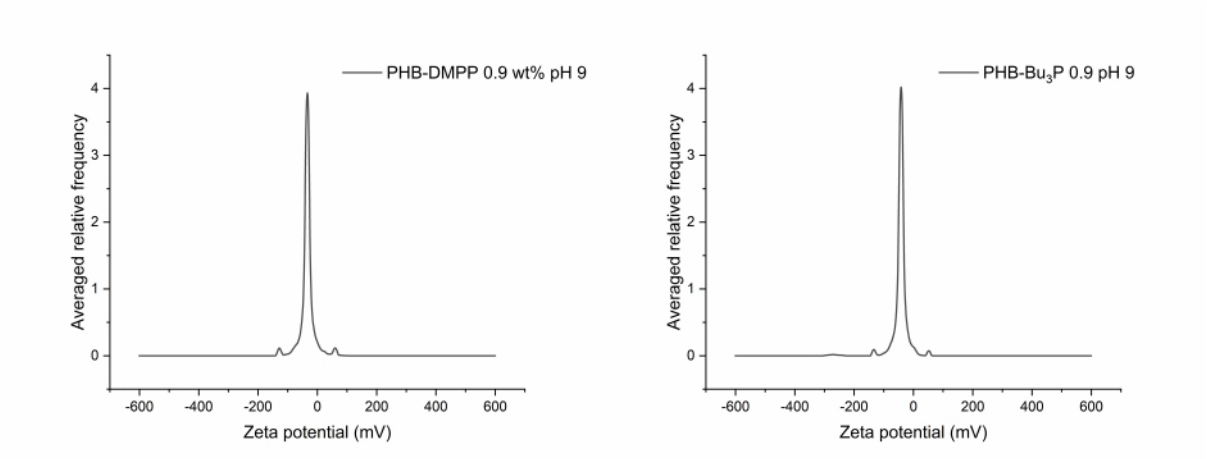

Figure S68:Zeta potential recorded for low molecular weight functionalised PHB measured in pH 9 0.9 wt% buffer solution.

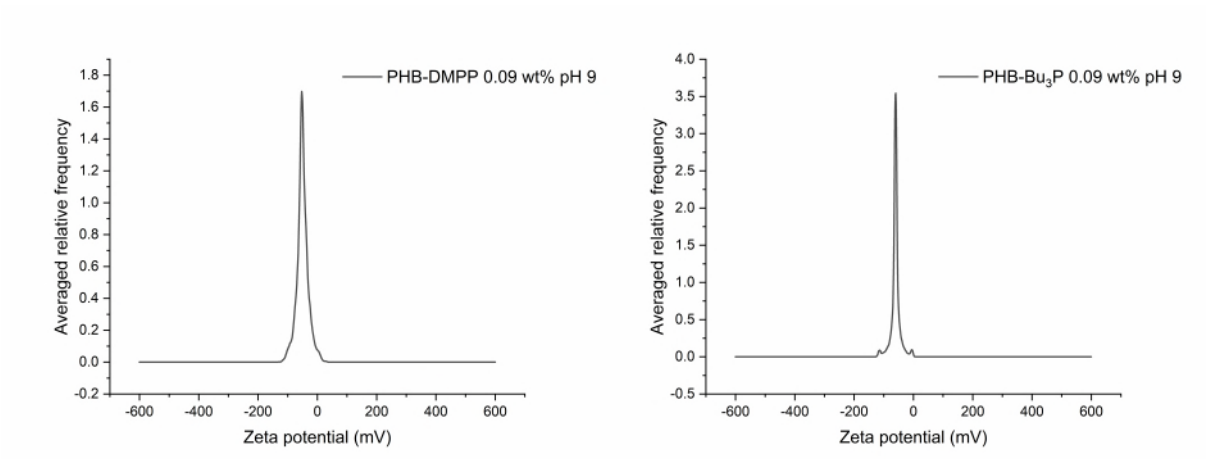

Figure S69:Zeta potential recorded for low molecular weight functionalised PHB measured in pH 9 0.09 wt% buffer solution.

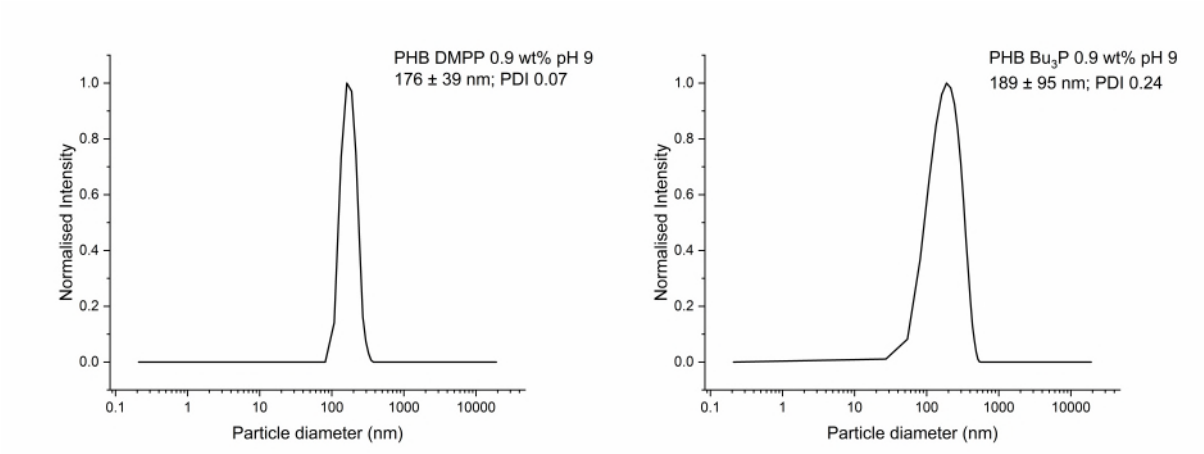

Figure S70: DLS recorded for low molecular weight functionalised PHB measured in pH 9 0.9 wt% buffer solution.

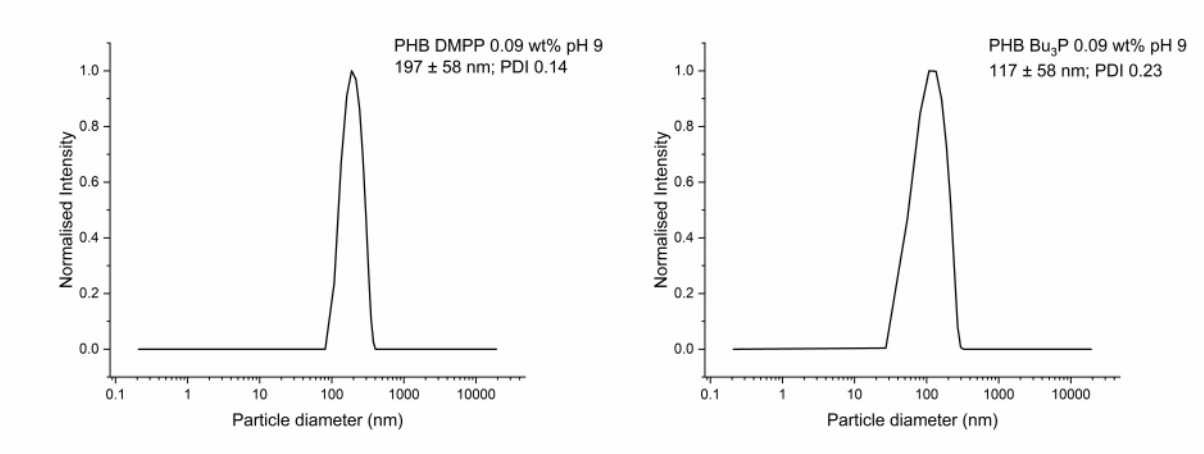

Figure S71: DLS recorded for low molecular weight functionalised PHB measured in pH 9 0.09 wt% buffer solution.

1.5 Degradation Experiment

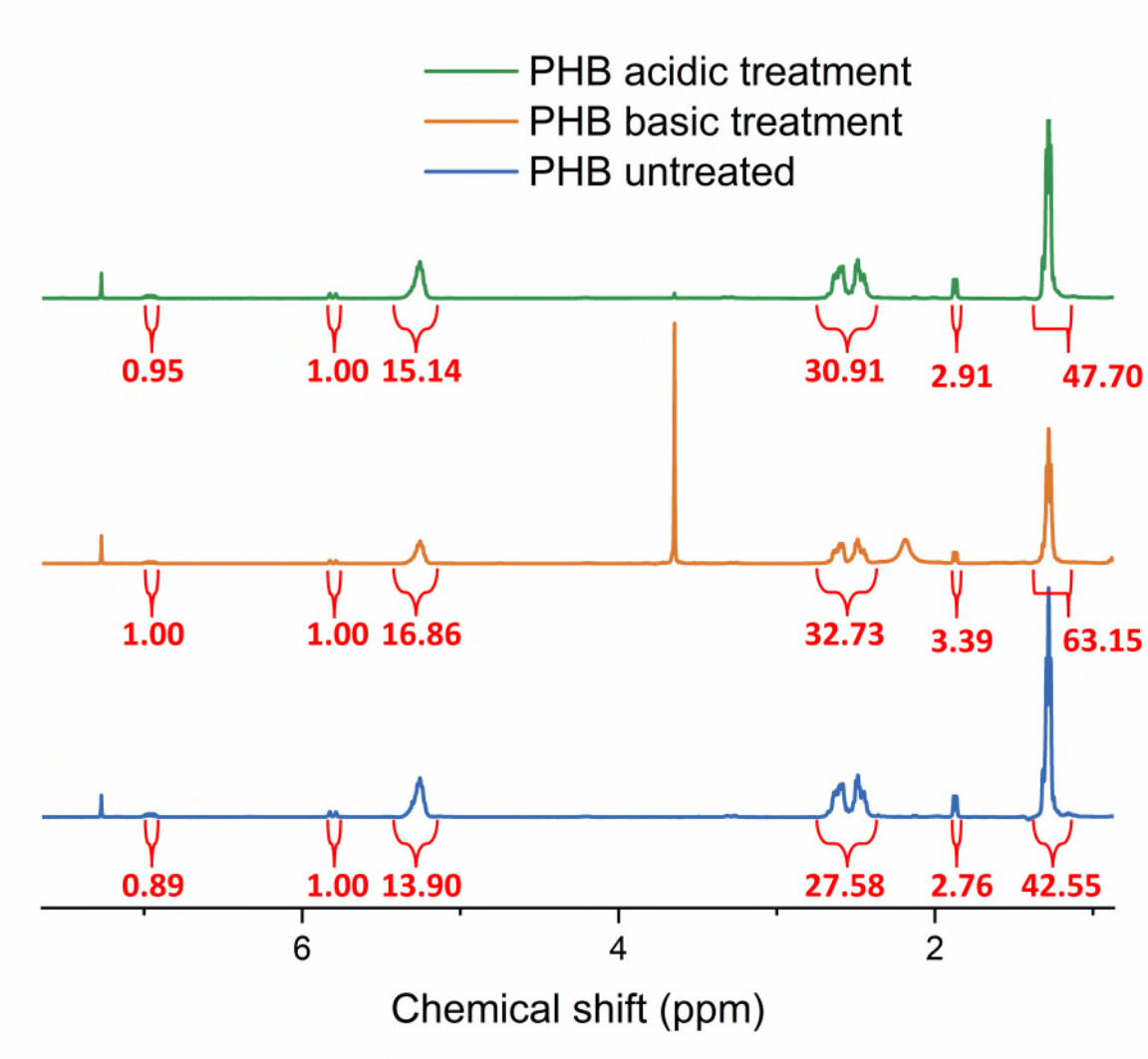

Figure S72: ^{1}H-NMR (400 MHz. $CDCl_3$) Comparison of untreated PHB to PHB treated with 0.9 wt% basic and acidic buffer. The Increase of the molecular weight is attributed to the loss of low molecular weight chains during purification of the samples.

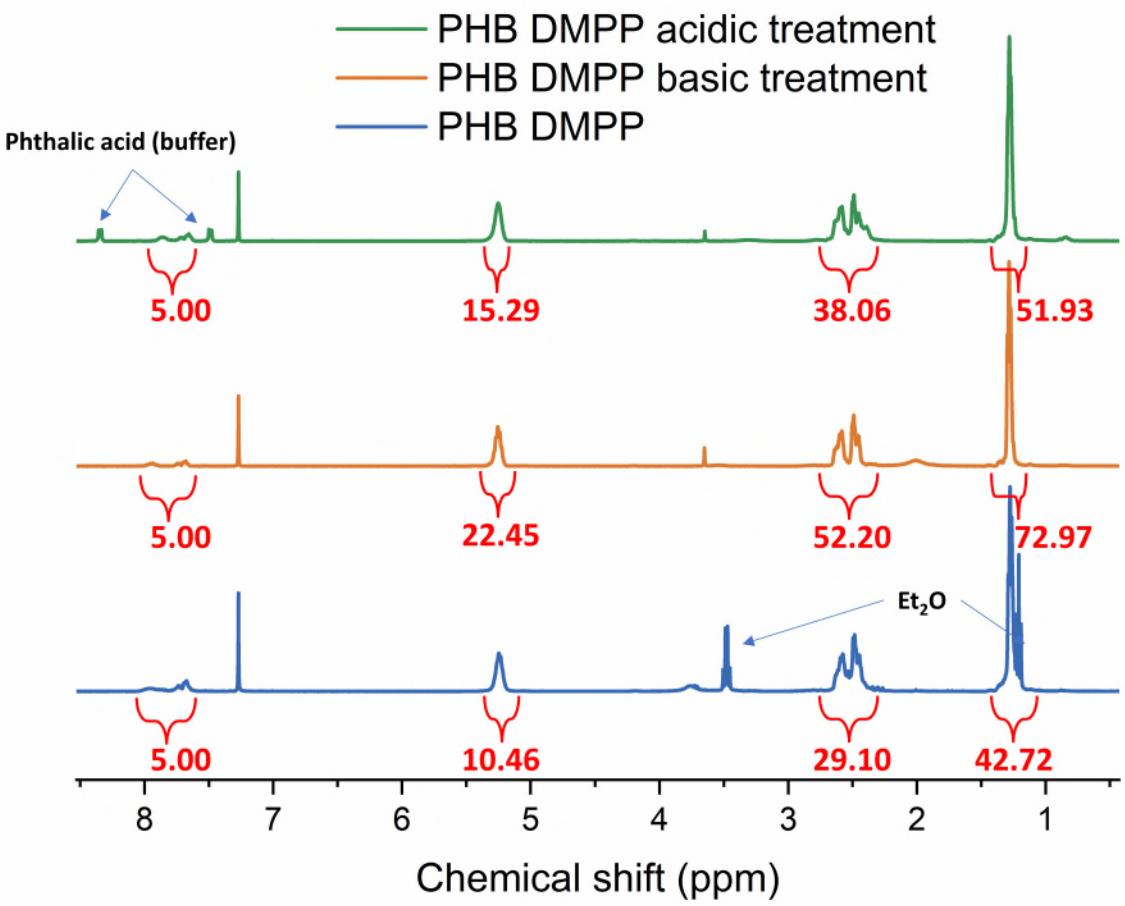

Figure S73: ^{1}H-NMR (400 MHz. $CDCl_3$) Comparison of untreated PHB-DMPP to PHB-DMPP treated with 0.9 wt% basic and acidic buffer. The Increase of the molecular weight is attributed to the loss of low molecular weight chains during purification of the samples.